

available at [www.sciencedirect.com](http://www.sciencedirect.com)journal homepage: [www.elsevier.com/locate/ejps](http://www.elsevier.com/locate/ejps)

## Identifying mechanisms of chronotolerance and chronoefficacy for the anticancer drugs 5-fluorouracil and oxaliplatin by computational modeling

Atila Altinok<sup>a</sup>, Francis Lévi<sup>b,c,d</sup>, Albert Goldbeter<sup>a,\*</sup>

<sup>a</sup> Unité de Chronobiologie Théorique, Faculté des Sciences, Université Libre de Bruxelles, Campus Plaine, C.P. 231, B-1050 Brussels, Belgium

<sup>b</sup> INSERM, U776, Rythmes Biologiques et Cancers, Villejuif F-94807, France

<sup>c</sup> Université Paris-Sud, UMR-S0776, Orsay F-91405, France

<sup>d</sup> Assistance Publique-Hôpitaux de Paris, Unité de Chronothérapie, Département de Cancérologie, Hôpital Paul Brousse, Villejuif F-94807, France

### ARTICLE INFO

Article history:

Published on line 11 November 2008

Keywords:

Circadian Rhythms  
Glutathione  
Chronotolerance  
Cell Cycle  
Cancer Chronotherapy  
Model

### ABSTRACT

We use an automaton model for the cell cycle to assess the toxicity of various circadian patterns of anticancer drug delivery so as to enhance the efficiency of cancer chronotherapy. Based on the sequential transitions between the successive phases G1, S (DNA replication), G2, and M (mitosis) of the cell cycle, the model allows us to simulate the distribution of cell cycle phases as well as entrainment by the circadian clock. We use the model to evaluate circadian patterns of administration of two anticancer drugs, 5-fluorouracil (5-FU) and oxaliplatin (l-OHP). We first consider the case of 5-FU, which exerts its cytotoxic effects on cells in S phase. We compare various circadian patterns of drug administration differing by the time of maximum drug delivery. The model explains why minimum cytotoxicity is obtained when the time of peak delivery is close to 4 a.m., which temporal pattern of drug administration is used clinically for 5-FU. We also determine how cytotoxicity is affected by the variability in duration of cell cycle phases and by cell cycle length in the presence or absence of entrainment by the circadian clock. The results indicate that the same temporal pattern of drug administration can have minimum cytotoxicity toward one cell population, e.g. of normal cells, and at the same time can display high cytotoxicity toward a second cell population, e.g. of tumour cells. Thus the model allows us to uncover factors that may contribute to improve simultaneously chronotolerance and chronoefficacy of anticancer drugs. We next consider the case of oxaliplatin, which, in contrast to 5-FU, kills cells in different phases of the cell cycle. We incorporate into the model the pharmacokinetics of plasma thiols and intracellular glutathione, which interfere with the action of the drug by forming with it inactive complexes. The model shows how circadian changes in l-OHP cytotoxicity may arise from circadian variations in the levels of plasma thiols and glutathione. Corroborating experimental and clinical results, the simulations of the model account for the observation that the temporal profiles minimizing l-OHP cytotoxicity are in antiphase with those minimizing cytotoxicity for 5-FU.

© 2008 Elsevier B.V. All rights reserved.

\* Corresponding author. Tel.: +32 2 650 5772; fax: +32 2 650 5767.

E-mail address: [agoldbet@ulb.ac.be](mailto:agoldbet@ulb.ac.be) (A. Goldbeter).

0928-0987/\$ – see front matter © 2008 Elsevier B.V. All rights reserved.

doi:10.1016/j.ejps.2008.10.024

## 1. Introduction

The circadian timing system controls the main pathways that are responsible for the pharmacokinetics (PK) and for the cellular metabolism and detoxification of anticancer medications. This confers chronopharmacological properties to these agents, i.e., dosing time dependencies in PK and pharmacodynamics (PD) (Lévi and Schibler, 2007). Circadian rhythms characterize most bioactivation and detoxification processes at transcription, protein, and enzymatic levels in the liver, the chief drug metabolizing organ, as well as in intestine, kidney, lung, etc. (Gachon et al., 2006). As a result, the circadian dosing time influences the extent of toxicity for 42 anticancer drugs, including cytostatics, cytokines, and “targeted biological agents” in laboratory mice or rats (Focan, 2003; Lévi, 2008). For all these drugs, the survival rate varies by 50% or more according to circadian dosing time of a potentially lethal dose. Such large differences in drug tolerance were observed irrespective of administration route or drug class (Haus et al., 1972; Hrushesky et al., 1982; Ohdo et al., 2001; Granda et al., 2002; Li et al., 2006). The purpose of this study is to investigate the effects of circadian rhythms on the chronopharmacology of anticancer drugs such as 5-fluorouracil and oxaliplatin.

Five-fluorouracil (5-FU) is an antimetabolite drug that substitutes for uracil in its physiological reactions and kills cells through such mechanism. The drug has a 10–20 min half-life in the plasma. The tolerability of a potentially lethal dose of 5-FU was 3–8-fold better in mice dosed in the early light span as compared to those receiving the drug at night. Best and worst dosing times were rather consistent among the different studies and investigators and corresponded to the early stage of the rest span and the middle of the activity span of the rest-activity circadian rhythm of the mice respectively (Popovic et al., 1982; Burns and Beland, 1984; Peters et al., 1987; Wood et al., 2006).

5-FU chronotolerance is governed by multiple rhythms in healthy target tissues, such as those in bone marrow, gut, skin and liver that are coordinated by the circadian timing system. Circadian rhythms have been shown for the enzymatic activities of dehydropyrimidine dehydrogenase, the rate-limiting enzyme which catabolizes 5-FU, orotate phosphoribosyl transferase, uridine phosphorylase and thymidine kinase, which are involved in the generation of the cytotoxic forms of 5-FU, and thymidilate synthase (TS), the main target enzyme of this antimetabolite (El Kouni et al., 1990; Naguib et al., 1993; Zhang et al., 1993; Porsin et al., 2003; Wu et al., 2004; Wood et al., 2006). Since TS is required for DNA synthesis, TS activity reaches its acme during the S-phase of the cell division cycle. As a result, the cell kill potential of 5-FU is by far the greatest for S-phase cells. Interestingly, the proportion of S-phase cells in mouse bone marrow is highest during darkness, corresponding to the usual span of mouse activity (Tampellini et al., 1998; Granda et al., 2005). Mechanisms of cell death result from p53-dependent apoptosis, a process that involves several rhythmic components (Granda et al., 2005; Gery et al., 2006). Furthermore, both p53 expression and apoptosis were downregulated by circadian disruption through *Per2* mutation, *Per1* knock out or chronic jet lag (Fu et al., 2002; Gery et al., 2006; Filipinski et al., 2005). Thus, the molecular interactions between the circadian

clock and the cell cycle and its related apoptosis pathways represent a major determinant of 5-FU chronotolerance.

On the contrary, oxaliplatin is an alkylating agent that forms DNA adducts, which in turn are responsible for cell death. Following administration, oxaliplatin irreversibly binds to plasma proteins while the free (unbound) fraction crosses the cellular membranes within minutes, resulting in triphasic plasma pharmacokinetics (Lévi et al., 2000). Oxaliplatin tolerability was enhanced ~3-fold in mice through drug administration near the middle of the dark span rather than at daytime (Boughattas et al., 1989). Best and worst dosing times corresponded to mid-activity and to mid-rest in the circadian rhythm in rest-activity, respectively. While no cell cycle phase specificity characterizes the cytotoxicity of oxaliplatin, the drug mostly arrests cycling cells at the G2/M transition, before they enter mitosis, resulting in cell cycle delay or cell death (Volland et al., 2006). Following intracellular entry, oxaliplatin irreversibly binds to thiol groups, such as reduced glutathione (GSH), a tripeptide that is present in the cytoplasm of most cells and shields the intracellular milieu from exposure to many toxicants, including oxaliplatin. Thus, the pronounced circadian rhythm in GSH is a major determinant of chronotolerance for oxaliplatin and other Pt complexes (Li et al., 1998).

Quite strikingly, the administration of a drug at the circadian time when it is best tolerated (chronotolerance) often achieves best antitumour activity (chronoefficacy), as demonstrated for 19 anticancer agents belonging to various classes (Focan, 2003; Lévi et al., 2007a,b; Lévi, 2008). This principle also applies to 5-FU and oxaliplatin. Thus, best antitumour efficacy was achieved in tumour-bearing mice receiving 5-FU in the early light (rest) span or oxaliplatin near the middle of the dark (activity) span (Peters et al., 1987; Granda et al., 2002). These experimental prerequisites have warranted the clinical development of chronotherapeutics with 5-FU and oxaliplatin. One of the goals of the present study will be to uncover the nature of factors that allow one to enhance at the same time chronotolerance and chronoefficacy of these anticancer drugs.

Human pharmacokinetics of 5-FU and oxaliplatin are also controlled by the circadian timing system, resulting in 24-h changes in the exposure of target tissues and tumours to these drugs (Nowakowska-Dulawa, 1990; Lévi et al., 2000). Circadian variations in plasma drug levels were found even despite continuous, constant-rate intravenous infusion of 5-FU (Petit et al., 1988). Inter-patient variability in circadian time-dependent PK has also been observed (Metzger et al., 1994). Of interest also is the finding that the activity of dihydropyrimidine dehydrogenase (DPD), the initial enzyme for the catabolism of 5-FU, in the peripheral blood mononuclear cells of diurnally active cancer patients varies significantly during the 24-h time period, with DPD activity being greatest between midnight and 4 a.m. (Harris et al., 1990; Zeng et al., 2005). Similarly, plasma glutathione (GSH) concentration also displayed a 24-h rhythm in cancer patients, with a maximum occurring near noon (Zeng et al., 2005). These results are consistent with prior ones on GSH concentration in human bone marrow (Smaaland et al., 2002). The GSH rhythm likely contributes to reduce oxaliplatin toxicity in the early afternoon.

The goal of this paper is to investigate mechanisms of chronotolerance and chronoefficacy for the anticancer drugs 5-FU and oxaliplatin by resorting to a computational approach.

We use an automaton model for the cell cycle to assess the cytotoxicity of various patterns of circadian administration of the two anticancer drugs. In Section 2 we present the cell cycle automaton model. Sections 3 and 4 are devoted to the cases of circadian administration of 5-FU and oxaliplatin, respectively. The results are discussed in Section 5 where we show the effect of combined administration of the two drugs according to distinct circadian schedules. Computational modeling allows us to identify conditions that simultaneously enhance the chronotolerance and chronoefficacy of anticancer drugs.

## 2. An automaton model for the cell cycle

Clinical and experimental studies can benefit from theoretical and numerical assistance to better understand the optimal delivery schedules of drug and the major parameters regulating chronotolerance and efficacy of some drugs (Goldbeter and Claude, 2002). To this end we need a model for the cell cycle. Instead of resorting to a detailed kinetic model of the sort proposed for the embryonic and yeast cell cycles, and currently developed for the mammalian cell cycle, we use here an automaton model that is not based on molecular details. This cell cycle automaton (CCA) model provides a simple phenomenologic description of the cell cycle in terms of transitions between sequential states corresponding to the successive phases of the cell cycle. The presence of anticancer drugs leads to probabilistic exit from the cell cycle, according to the drug concentration. A random component is introduced in the cell cycle automaton to take into account the variability of transitions between cell cycle phases in a proliferating cell population (Smith and Martin, 1973; Brooks et al., 1980; Cain and Chau, 1997). In addition to circadian control, the cell cycle automaton can readily be used to investigate the impacts of different temporal patterns of drug administration.

The major effect of anticancer drugs interfering with the cell cycle is to block cells in a specific phase before cell death. The antimetabolite 5-FU disorganizes pyrimidine metabolism in cells undergoing DNA replication, and is therefore toxic for cells in S phase. Conversely, alkylating agents such as oxaliplatin exert their effects in all phases of the cell cycle. The CCA model can nevertheless be used also for oxaliplatin, with results that will be compared with those obtained for 5-FU.

### 2.1. Rules of the automaton model

The automaton model for the cell cycle, schematized in Fig. 1, is based on the following assumptions. Proliferating cells progress through 4 successive phases of the cell cycle: G1, S (DNA replication), G2, and M (mitosis). After mitosis during the M phase, a cell divides into two cells in G1 phase (the G0 phase is not considered here). In the model, each phase is determined by the mean duration in which cells spend time, and the variability of this duration around the mean value in a whole population. When a cell ends its time in a phase of the cell cycle, the transition to the next one occurs. A new residence time in the new phase is calculated in a random

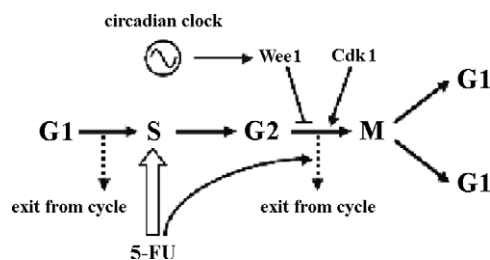


**Fig. 1 – Scheme of the automaton model for the cell cycle and effect of 5-FU.** The cell passes through four successive phases of the cell cycle: G1, S (DNA replication), G2 and M (mitosis). After completing an entire cycle, two cells enter the cycle at the beginning of G1. The residence time in a particular phase is calculated at each transition into that phase, according to a distribution centered around a mean duration  $\pm$  a given variability in this duration (% of the mean value). The cell possesses a certain propensity to exit the cell cycle at the G1/S or G2/M transitions, which leads to cell death. The cell cycle is regulated by the circadian clock through the kinases WEE1 and CDK1, which inhibit or induce the G2/M transition, respectively. Cells exposed in S phase to the anticancer drug 5-FU have an increased propensity to quit the proliferating pool at the nearest G2/M transition.

manner according to the mean value and the variability. In the case of a uniform probability distribution, the duration varies in the interval  $[D(1 - V), D(1 + V)]$ , where  $D$  is the mean duration and  $V$  the variability (expressed in % of the mean value).

At each time step, the cells have a certain probability to exit the proliferating pool at the next G1/S or G2/M transition. To reach population homeostasis, i.e. the maintenance of the total cell number within a range of oscillations, we further assume the balance between cell replication due to mitosis and exit from the proliferating pool. During the time of one cell cycle, two cells emerge from one cell, and the homeostasis is reached when 50% of cells exit the cell cycle during that time. When this probability is higher, the cell population decreases exponentially. Conversely, a smaller value for the probability of exiting the cell cycle corresponds to an exponential increase of the population. The use of a logistic equation allows us to maintain the total cell number in a prescribed range (see Appendix A.2). The automaton model for the cell cycle will be used to describe the dynamic behavior of a population of proliferating cells subjected to entrainment by the circadian clock and to the administration of anticancer drugs such as 5-FU or oxaliplatin.

5-FU is toxic for cells in DNA replication during the S phase. The effect of this drug is incorporated into the model only for cells in S phase in presence of the drug. Following the drug concentration, cells in S phase in presence of 5-FU have an increased propensity to quit the proliferating pool at the next G2/M transition. In contrast, l-OHP affects cells in all phases of the cell cycle. Regardless of their current phase, cells exposed to the drug have an increased propensity to quit the cycle at the next G1/S or G2/M transition.

## 2.2. Dynamics of the automaton model: repetitive transitions between cell cycle phases

The variability in the duration of the cell cycle phases is responsible for progressive cell desynchronization. In the absence of variability, if the duration of each phase is the same for all cells, the population behaves as a single cell. Then, if all cells start at the same point of the cell cycle, e.g., at the beginning of G1, a sequence of square waves bringing the cells synchronously through G1, S, G2, M, and back into G1 occurs (Altinok and Goldbeter, in preparation). The drop in cell number at the end of the G1 and G2 phases reflects the assumption that exit from the cell cycle occurs at these transitions, to counterbalance the doubling in cell number at the end of M. These square waves will continue unabated over time. However, as soon as some degree of variability of the cell cycle phase durations is introduced, the square waves transform into oscillations through the cell cycle phases, the amplitude of which diminishes as the variability increases. In the long term, these oscillations dampen as the system settles into a steady state distribution of cell cycle phases: the cells are fully desynchronized and have forgotten the initial conditions (Altinok and Goldbeter, in preparation).

## 2.3. Coupling the cell cycle automaton to the circadian clock

To determine the effect of circadian rhythms on anticancer drug administration, it is important to incorporate the link between the circadian clock and the cell cycle. Entrainment by the circadian clock can be included in the automaton model by considering that the protein WEE1 undergoes circadian variation due to induction by the circadian clock proteins CLOCK and BMAL1 of the expression of the *Wee1* gene (Matsuo et al., 2003; Hirayama et al., 2005; Reddy et al., 2005) (see Fig. 1). WEE1 is a kinase that phosphorylates and thereby inactivates protein kinase CDC2 (also known as the cyclin-dependent kinase CDK1) that controls the transition G2/M and, consequently, the onset of mitosis.

In mice subjected to a 12:12 light-dark cycle (12 h of light followed by 12 h of darkness), WEE1 level rises during the second part of the dark phase, i.e., at the end of the activity phase. Humans generally keep a pattern in which 16 h of diurnal activity are followed by 8 h of nocturnal sleep. Therefore, when modeling the link between the cell cycle and the circadian clock in humans, we will consider a 16:8 light-dark cycle (16 h of light, from 8 a.m. to 12 p.m., followed by 8 h of darkness, from 12 p.m. to 8 a.m.) (Bjarnason and Jordan, 2000; Bjarnason et al., 2001; Lévi, 2001; Granda and Lévi, 2002) (Fig. 2). To keep the pattern corresponding to the situation in mice (with a 12-h shift due to the change from nocturnal to diurnal activity) and in agreement with observations in human cells (Bjarnason et al., 2001), the rise in WEE1 should occur at the end of the activity phase, i.e., with a peak at 10 p.m. The decline in WEE1 activity is followed by a rise in the activity of the kinase CDK1, which enhances the probability of transition to the M phase. We thus shall consider that the rise in WEE1 is immediately followed by a similar rise in CDK1 (see Fig. 4).

In the cell cycle model, we will consider that the probability of transition from G2 to M, at the end of G2, decreases as WEE1 rises, according to Eq. (1). Conversely, we shall assume that the probability of premature transition from G2 to M (i.e., before the end of G2, the duration of which was set when the automaton entered G2) increases with the activity of CDK1 according to Eq. (2). The probability is first determined with respect to CDK1; if the G2/M transition has not occurred, the cell progresses in G2. Only at the end of G2 is the probability of transition to M determined as a function of WEE1

$$P(\text{transition}(G2 \rightarrow M)) = 1 - k_w [WEE1] \quad (1)$$

$$P(\text{transition}(G2 \rightarrow M)) = k_c [CDK1] \quad (2)$$

In a previous study (Altinok et al., 2007a) we described the rise in WEE1 and CDK1 by a step increase lasting 4 h. Here, instead of such a square-wave pattern, we will use a temporal pattern of semi-sinusoidal shape. Thus, we assume that WEE1 increases in a semi-sinusoidal manner between 4 p.m. and 4 a.m., with a peak at 10 p.m., while CDK1 increases in the same manner between 10 p.m. and 10 a.m., with a peak at 4 a.m. (Fig. 4) (Altinok et al., 2007b).

Upon entrainment by the circadian clock, cells become more synchronized than in the absence of entrainment. In the case considered in Fig. 2, the period changes from 22 to 24 h, which corresponds to the period of the external light-dark cycle. When the variability is nil, we observe that the fraction of cells in S phase decreases to zero at the trough of the oscillations. This does not occur when variability is higher, e.g., 15% (Fig. 2E). The fraction of S-phase cells then oscillates with reduced amplitude, reflecting again the effect of cell cycle desynchronization. However, in contrast to the progressive dampening of the oscillations in the absence of entrainment, when the cell cycle automaton is driven by the circadian clock oscillations appear to be sustained (Altinok et al., 2007a,b).

## 3. Circadian administration of 5-FU

### 3.1. Mechanism of action of 5-fluorouracil

Cells exposed in S phase to 5-FU arrest in this phase as a result of thymidylate synthase inhibition; then, they progress through the cell cycle or die through p53-dependent or independent apoptosis (Lévi, 1997). In the model we will consider that cells exposed to 5-FU while in the S phase have an enhanced propensity of quitting the proliferative compartment at the next G2/M transition (Fig. 1). The propensity  $P$  (in  $\text{min}^{-1}$ ) of quitting the cycle will be taken as proportional to the 5-FU concentration,  $[5\text{-FU}]$ , according to Eq. (3):

$$P = P_0(1 + k_f[5\text{-FU}]) \quad (3)$$

We assume that the basal exit propensity in the absence of 5-FU,  $P_0$  (in  $\text{min}^{-1}$ ) is multiplied by a factor of 20 when the level of 5-FU, which varies from 0 to 100 in acu (arbitrary concentration units) reaches its maximum value. Thus we will take the value  $k_f = 0.19 \text{ acu}^{-1}$ . Other hypotheses might be retained for the dose-response curve of the drug. Thus, larger or smaller

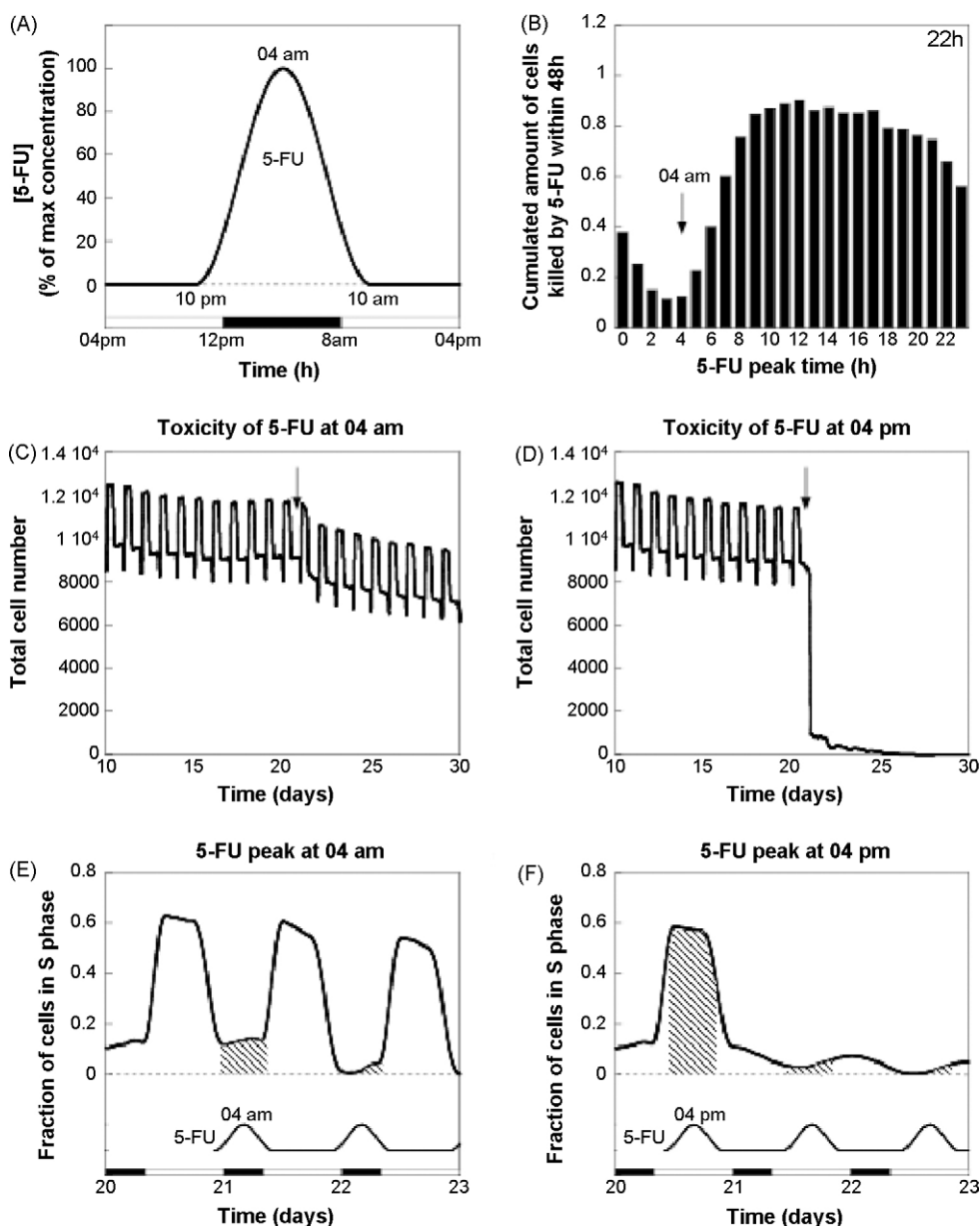


**Fig. 2** – Effect of circadian administration of 5-FU. (A) Semi-sinusoidal profile of 5-FU administration. The temporal pattern is similar to that used clinically: the peak time occurs during the dark phase at 4 a.m. and no administration occurs between 10 a.m. and 10 p.m. Cells exposed to the drug in S phase have an increased propensity to quit the proliferating pool, according to the linear relationship given by Eq. (3), with  $k_f = 0.19 \text{ acu}^{-1}$ . This value ensures that at the maximum level of [5-FU], the propensity of exiting the cycle is multiplied by a factor of 20. (B) Cumulated amount of cells (in units of  $10^4$  cells) killed within 48 h by 5-FU, as a function of the peak time of circadian 5-FU administration. The cell cycle duration here equals 22 h. Minimum toxicity is then observed around a peak time close to 3–4 a.m. (C) Evolution of the total cell number upon circadian administration of 5-FU with a peak time at 4 a.m. Circadian drug delivery begins at day 20 until day 30. The cell population displays only a slight decrease due to exposure to the drug. (D) Evolution of the total cell number upon circadian administration of 5-FU with a peak time at 4 p.m. Circadian drug delivery begins at day 20 until day 30. In this case, the drug kills the major part of the cell population within 2 days. Prior to entrainment the cell cycle duration is 22 h, with a variability  $V = 10\%$ . (E) Time evolution of the fraction of cells in S phase upon circadian administration of 5-FU with a peak time at 4 a.m. (F) Time evolution of the fraction in S phase upon circadian administration of 5-FU with a peak time at 4 p.m. The peak in 5-FU coincides with the maximum in the fraction of cells in S phase. Hence the toxicity of the drug is much larger than in the case of (E) where the peak in 5-FU coincides with the minimum fraction of cells in S phase. In (F) most cells are killed in the first day of drug administration. Prior to entrainment the cell cycle duration is 22 h, with a variability  $V$  of 15%. As in subsequent figures (except Fig. 11 and Fig. 12C and D; see Annex A.4(C)) numerical simulations are performed with  $10^4$  cells starting from the steady-state distribution of cell cycle phases. This means that, initially, cells start in different phases and at different times, which are randomly distributed according to the steady-state proportions of cell cycle phases.

slopes of the linear relationship will respectively correspond to stronger or weaker cytotoxic effects of 5-FU. A threshold dependence may also be introduced, in which case the relationship takes the form of a sigmoidal curve that tends to a step function as the steepness of the threshold increases. For simplicity, because the half-life of 5-FU is short, of the order of minutes, we shall assume that the effective concentration of 5-FU closely follows the circadian pattern imposed by drug delivery.

### 3.2. Effect of the peak time of circadian administration of 5-FU

The main prediction from the CCA model is that there exists a marked circadian effect in 5-FU cytotoxicity. We have considered the effect of a circadian pattern of 5-FU delivery such that over a period of 24 h, no 5-FU is administered during 12 h, while a semi-sinusoidal delivery occurs over the remaining 12 h. This pattern is illustrated in Fig. 2A in the case where the peak circadian delivery occurs at 4 a.m., which is the temporal pattern used clinically (Lévi et al., 1994, 1997). We will use a similar pattern to determine the effect of changing the time for maximum drug delivery.

Shown in Fig. 2B is the cumulated amount of cells killed by 5-FU in a given time (48 h) as a function of the peak time of circadian delivery of the drug. We observe that cytotoxicity is minimum when the peak time is around 3–4 a.m., and maximum when the peak time is in the range 10 a.m. to 6 p.m. These results are obtained when the cell cycle length is of 22 h. As will be shown in Fig. 3 below, the outcome of the numerical simulations depends on the cell cycle duration.

Another illustration of the effect of the peak time of 5-FU delivery is shown in Fig. 2C and D where the time course of the total number of cells after the beginning of the treatment by 5-FU (at the time indicated by the vertical arrow) is plotted for circadian 5-FU delivery peaking at 4 a.m. and 4 p.m., respectively. Drastic differences in cytotoxicity can be observed: the effect is minimal when 5-FU peaks at 4 a.m. while the cytotoxicity of the drug is extremely large when circadian drug delivery peaks at 4 p.m. Indeed, the drop in total number of cells is very steep and largely occurs during the first day of treatment. The two distinct peak times correspond to points close to the minimum and maximum cytotoxicity in the histogram in Fig. 2B.

The model provides an explanation for the change in cytotoxicity according to the peak time of circadian 5-FU delivery. When the CCA model is entrained by the circadian clock, the fraction of cells in S phase passes through a maximum during the light phase and through a minimum during the dark phase. The phase of the entrained cell cycle is determined by the time at which the peaks in WEE1 and CDK1 occur; these peak times are in turn set by the time at which BMAL1 reaches its maximum during the day.

When 5-FU delivery peaks at 4 a.m., the peak in 5-FU occurs at a time where the fraction of cells in S phase is minimum (Fig. 2E). The cytotoxicity of the drug is then weak, since relatively few cells are in the phase sensitive to 5-FU. In contrast, cytotoxicity is much larger when 5-FU peaks at 4 p.m. (Fig. 2F) because the peak of the drug occurs precisely when the fraction of cells in S phase passes through a maximum.

Intermediate cytotoxicities are observed when the peak times of 5-FU occur, for example, at 10 a.m. or 10 p.m. (see also Fig. 2B). Indeed, the peak in 5-FU then partly overlaps with the peak in the fraction of cells in S phase. When the infusion of 5-FU becomes continuous, there is always an overlap with the fraction of cells in S phase. The cytotoxicity of the drug is then close to that observed for the most cytotoxic circadian patterns, e.g., that peaking at 4 p.m.

### 3.3. Effect of variability of cell cycle phase durations

Cytotoxicity of 5-FU is markedly affected by the degree of variability  $V$  of duration of the cell cycle phases. Thus, for the circadian pattern peaking at 4 a.m., which is the least cytotoxic when cell cycle duration is of 22 h, the data indicate that cytotoxicity rises when the degree of variability increases (see Fig. 10A, in the section comparing the effect of 5-FU with those of oxaliplatin). When variability increases, the cells indeed desynchronize more rapidly so that at any moment in time the fraction of cells in S phase—thus sensitive to 5-FU—is larger than in the case where cells are better synchronized, at relatively smaller values of variability (Lévi et al., 2008).

### 3.4. Effect of cell cycle length

The marked dependence on cytotoxicity on the circadian pattern of 5-FU delivery shown in Fig. 2B was obtained when the cell cycle length is 22 h. This dependence changes with the duration of the cell cycle. Numerical simulations of the CCA model at different values of the cell cycle length indeed show that a minimum in 5-FU cytotoxicity only occurs when the cell cycle duration ranges from 18 to 26 h. Moreover, panels B–F in Fig. 3 indicate that the minimum progressively shifts from 12 p.m. to 1 a.m., 3 a.m., 5 a.m., and 12 a.m. when the duration of the cell cycle increases from 18 to 26 h. The depth of the trough, which corresponds to reduced cytotoxicity, is most significant when the duration of the cell cycle ranges from 20 to 24 h (Fig. 3C–E). When the cell cycle length is 16 h, no minimum is apparent (Fig. 3A), while for a cell cycle duration of 26 h, the minimum in 5-FU cytotoxicity as a function of peak time in circadian delivery becomes very shallow.

To clarify the reasons for the dependence of the circadian cytotoxicity profile of 5-FU as a function of cell cycle duration, it is useful to plot the time evolution of the fraction of cells in S phase for cell cycle durations of 16 h (Fig. 4A), 22 h (Fig. 4B) and 26 h (Fig. 4C). In these panels, the 5-FU profile peaking at 4 a.m. is shown as a dashed line, because cells are not actually exposed to the drug; hence there is no drop in the fraction of cells in S phase after each peak of 5-FU, as was the case in Fig. 2E and F. When the cell cycle length is of 16 h, we observe three peaks of cells in S phase over a 24-h period. As a result, the fraction of cells in S phase always remains at a relatively large value, so that the cytotoxicity of 5-FU would be large over the whole 24-h period (see Fig. 3A), in contrast to what is observed when the cell duration is of 22 h (see Fig. 3D).

When the cell duration is 26 h, the cell cycle is entrained by the circadian clock but the waveform of the fraction of cells in S phase is much smoother, with a mild trough, compared to the case when the cell cycle length is 22 or 24 h. As a result,

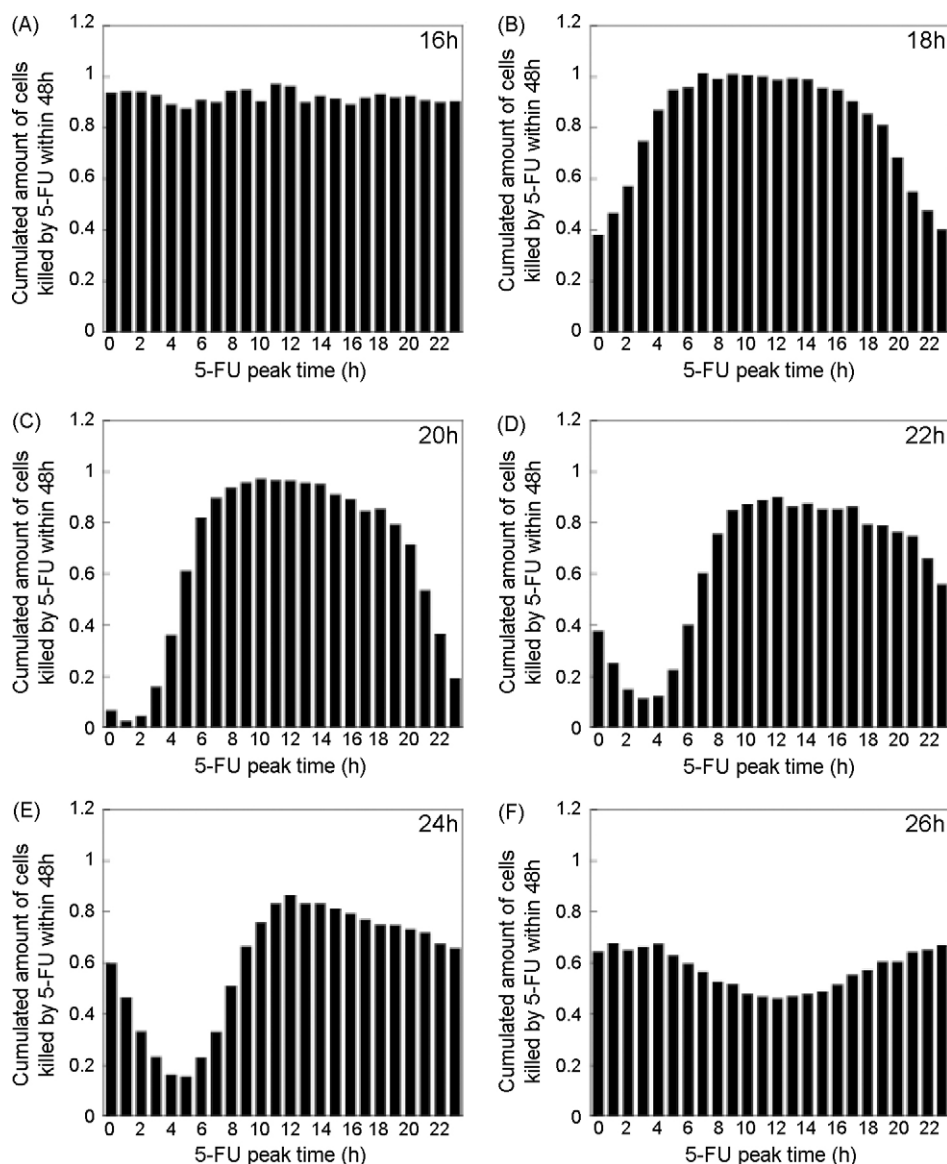


**Fig. 3 – Cytotoxicity of 5-FU as a function of peak time of circadian administration of the anticancer drug. The cumulated amount of cells (in units of  $10^4$  cells) killed by 5-FU (i.e. all cells that have quitted the cell cycle owing to 5-FU) within 48 h is shown as a function of the peak time of circadian 5-FU administration for various durations of the cell cycle prior to entrainment: (A) 16 h, (B) 18 h, (C) 20 h, (D) 22 h, (E) 24 h, or (F) 26 h. The histograms are established for a variability  $V = 10\%$ . A significant minimum in drug toxicity appears for cell cycle durations between 18 and 24 h. The position of this minimum depends on the cell cycle duration.**

the amount of cells killed by 5-FU varies less as a function of the time of the circadian peak in 5-FU.

#### 4. Circadian administration of oxaliplatin

##### 4.1. Mechanism of action of oxaliplatin and protection by plasma thiols and glutathione

Oxaliplatin (l-OHP) damages cells by binding irreversibly to DNA and forming inter- and intra-strand bridges. In contrast to 5-FU, the cytotoxicity of l-OHP is not specific to any particular cell cycle phase. What is specific, however, is the capacity

of l-OHP to form complexes with compounds such as plasma thiols (PSH) and cellular glutathione (GSH). Once complexed with either PSH or GSH, l-OHP loses its activity. Both PSH and GSH display circadian variations. We will thus consider that the propensity  $P$  of quitting the proliferative cycle will increase in the presence of l-OHP, regardless of the phase in which the cell is exposed to the drug (Fig. 5), according to Eq. (4):

$$P = P_0(1 + k_{ox}[l\text{-OHP}]) \quad (4)$$

Here we will consider that at the maximum l-OHP concentration  $[l\text{-OHP}]_{\max} = 100$  (in arbitrary concentration units, acu), the propensity of quitting the cycle at the G1/S or

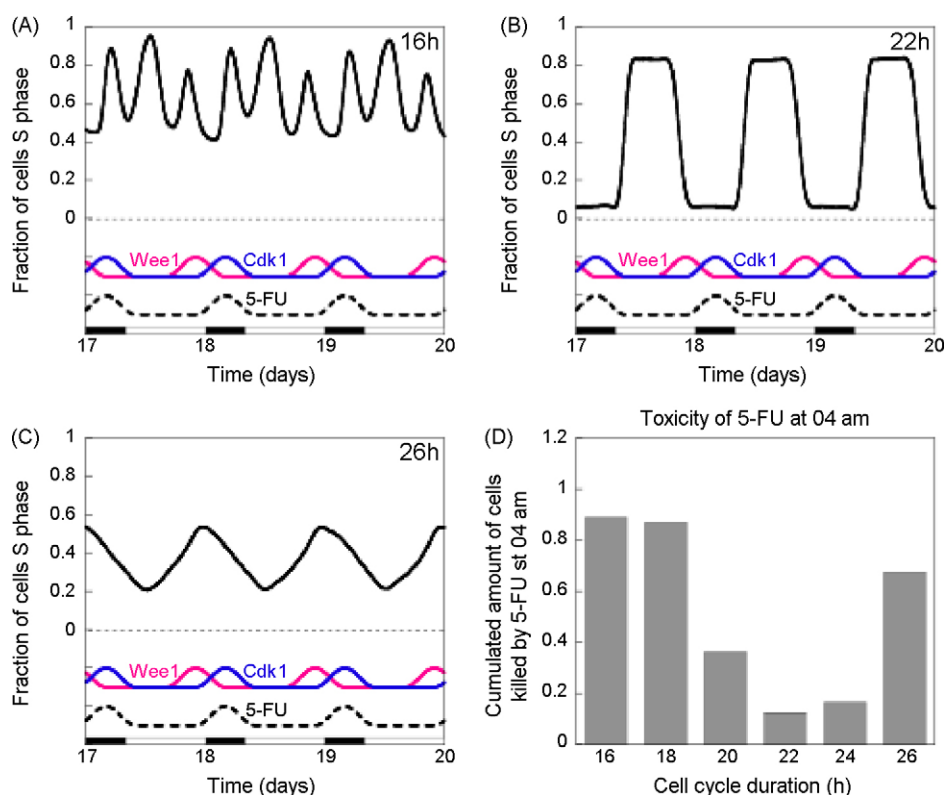


**Fig. 4 – Evolution of the fraction of cells in S phase and effect of 5-FU circadian administration as a function of cell cycle duration. (A)–(C)** Temporal variation of the proportion of cells in S phase for a cell cycle of 16 h (A), 22 h (B) and 26 h (C) subjected to circadian entrainment mediated by WEE1 and CDK1 (red and blue curves at bottom of each panel). The curves are established by numerical simulation of the cell cycle automaton model with a variability  $V = 10\%$ . The curves are obtained in the absence of 5-FU, but the circadian pattern of 5-FU administration peaking at 4 a.m. is shown (dashed line) to illustrate the potential cytotoxic effect of this drug delivery pattern on cells in S phase. The cell cycle of 16 h-period is more difficult to entrain to 24 h, leading to three peaks in the fraction of cells in S phase. (D) The distinct profiles of the oscillations of the fraction of cells in S phase result in different levels of cytotoxicity for the circadian pattern of 5-FU administration peaking at 4 a.m. (For interpretation of the references to colour in this figure legend, the reader is referred to the web version of the article.)

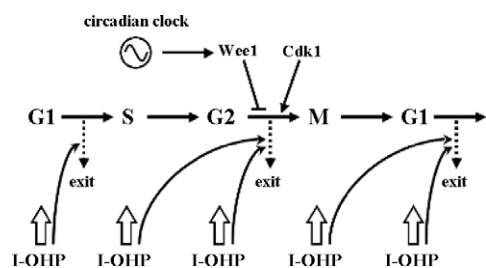


**Fig. 5 – Scheme of the cell cycle automaton model and for effect of oxaliplatin.** The mechanism of the cell cycle automaton and the entrainment by the circadian clock are as described in Fig. 1. In contrast to the action of 5-FU, oxaliplatin (l-OHP) does not affect a single, specific phase of the cell cycle. All cells in each phase are vulnerable to this anticancer drug. At the maximum l-OHP concentration the presence of oxaliplatin increases by a factor of ten the propensity to quit the proliferating pool for cells exposed to the drug in any phase of the cell cycle. Exit from the cell cycle following exposure to l-OHP occurs at the nearest G1/S or G2/M transition, with a propensity given by Eq. (4).

G2/M transitions is multiplied by a factor of ten. Thus we take  $k_{ox} = 0.09 \text{ acu}^{-1}$ . This value ensures that the cumulated increase in the propensity of quitting the cycle upon exposure to l-OHP is of the same order as the increase retained for 5-FU.

We further consider the binding of l-OHP to plasma thiols and cellular glutathione (Fig. 6A and B). The consequence of the formation of these inactive complexes is to decrease the net amount of free l-OHP able to carry out its cytotoxic action. The binding of blood l-OHP (l-OHPb) to plasma thiols (PSHb) will result in the formation of complex B, while the binding of cellular l-OHP (l-OHPc) to cellular glutathione (GSHc) will result in the formation of complex C. Remaining cellular l-OHP (l-OHPd) will represent the available free cytotoxic form of the drug leading to cell death through the formation of bridges within and between DNA strands. The kinetic equations corresponding to the scheme of Fig. 6B are given in Appendix A.

We will examine the effect of circadian administration of l-OHP by which the drug is delivered in a semi-sinoidal manner during 12 h, followed by cessation of drug delivery for the following 12 h. Illustrated in Fig. 7A is the case where the circa-

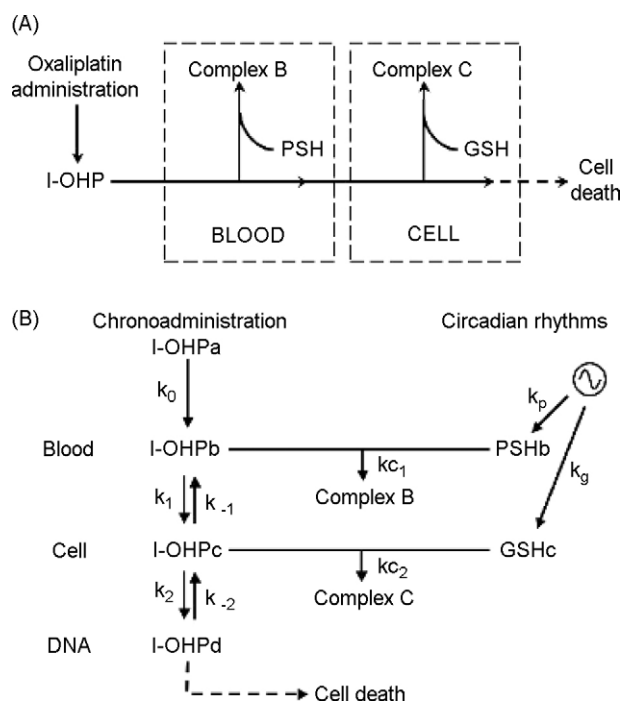


**Fig. 6 – Scheme showing the reduction in the cytotoxicity of oxaliplatin due to the formation of complexes with plasma thiols (PSH) and cellular glutathione (GSH). (A) Oxaliplatin is administered into the blood compartment. Plasma thiols (PSH) form inactive, irreversible complexes (complex B) with the drug. Free oxaliplatin enters the cellular compartment, where glutathione (GSH) in turn forms an inactive, irreversible complex (complex C) with I-OHP. The remaining free oxaliplatin leads to toxicity in the cell, by forming inter- and intra-strand bridges in DNA. (B) Detailed sequence of reactions leading to the formation of complexes of I-OHP with PSH and GSH. The system is described by a set of kinetic equations given in Appendix A.**

dian pattern of I-OHP administration peaks at 4 p.m., which is the clinically used pattern for I-OHP. The goal of our analysis is to determine how the cytotoxicity of I-OHP varies according to the peak time of its circadian administration. Other aspects to be investigated are the effect of cell cycle variability and the influence of the duration of the cell cycle. These issues will be addressed by taking into account the circadian variation of PSHb and GSHc, which peaks at 4 p.m. and 12 p.m., respectively (Fig. 7B). The choice of the particular circadian profiles is based on experimental observations (Bridges et al., 1992; Li et al., 1998).

#### 4.2. Effect of peak time of circadian administration of oxaliplatin

A first indication that the cytotoxicity of I-OHP depends on the circadian pattern of drug administration is presented in Fig. 7C and D. We observe that in contrast to the case of 5-FU, here the cytotoxicity is more pronounced when peak circadian delivery of I-OHP occurs at 4 a.m. rather than at 4 p.m. This result is predicted by the model even though I-OHP affects all phases

of the cell cycle in a similar way. Such a dependence of cytotoxicity on the temporal pattern of I-OHP delivery originates from the existence of circadian variations in plasma thiols and cellular glutathione.

In Fig. 8 we compare the temporal profiles of I-OHP present in blood (I-OHPb) and in cells (I-OHPc), and available for damaging the cells (I-OHPd) when the circadian pattern of administered oxaliplatin (I-OHPa) peaks at 4 a.m. (Fig. 8A) or 4 p.m. (Fig. 8B). The amount of oxaliplatin in the effective cytotoxic form I-OHPd is smaller at 4 p.m. than at 4 a.m. This difference results from the circadian profiles of PSHb and GSHc (Fig. 7B). These profiles are such that complex C forms more abundantly when I-OHP peaks at 4 a.m. while complex B forms preferentially when I-OHP peaks at 4 p.m. (Fig. 8C and D). Because the effect of plasma thiols seems predominant compared to that of glutathione, the remaining, free form I-OHPd is more abundant when I-OHP peaks at 4 a.m. This is the reason why the circadian delivery pattern peaking at 4 a.m. is more cytotoxic than the pattern peaking at 4 p.m., as shown in Fig. 7C and D.

Plotted in Fig. 9 is the histogram showing the cumulated cytotoxicity within 48 h as a function of the peak time of circadian I-OHP delivery, when the cell cycle duration is of 16 h (A), 22 h (B), and 26 h (C). Among the three cases considered, the clearest occurrence of a minimum in the cytotoxicity profile is observed when the cell cycle length is of 22 h. Then the minimum occurs when the peak in drug delivery is around 6–7 p.m. The minimum is more shallow but occurs around the same time for the other two values of the cell cycle duration. We show in Fig. 9D a comparison of the cytotoxicity of the pattern of I-OHP delivery peaking at 4 p.m. when the cell cycle duration ranges from 16 to 26 h. The cytotoxicity is minimum for cell cycle durations around 20 h, but the variation is more reduced than in the case of circadian delivery of 5-FU (see Fig. 3).

#### 4.3. Effect of variability in duration of cell cycle phases

The cell cycle automaton model indicates that variability in the duration of cell cycle phases represents yet another factor that can modulate the cytotoxicity of anticancer drugs. Numerical simulations of the CCA model reveal a difference in this respect between the cases of 5-FU and I-OHP. Whereas an increase in variability is accompanied by increased cytotoxicity in the case of 5-FU (Fig. 10A), it does not have much effect on cytotoxicity in the case of I-OHP (Fig. 10B). In each panel of Fig. 10 established for a cell cycle of 22 h entrained by the circadian clock, the delivery pattern considered corresponds to nearly minimum cytotoxicity in these conditions, namely it peaks at 4 a.m. for 5-FU and at 4 p.m. for I-OHP.

## 5. Discussion

Searching for the most appropriate timing for drug administration is the goal of chronotherapeutics. Such an approach has been pursued for long in the treatment of cancer, and is based on both experimental studies in animals and clinical trials, which are still ongoing. In particular cancer chronotherapeutics aims at taking into account the influence of circadian

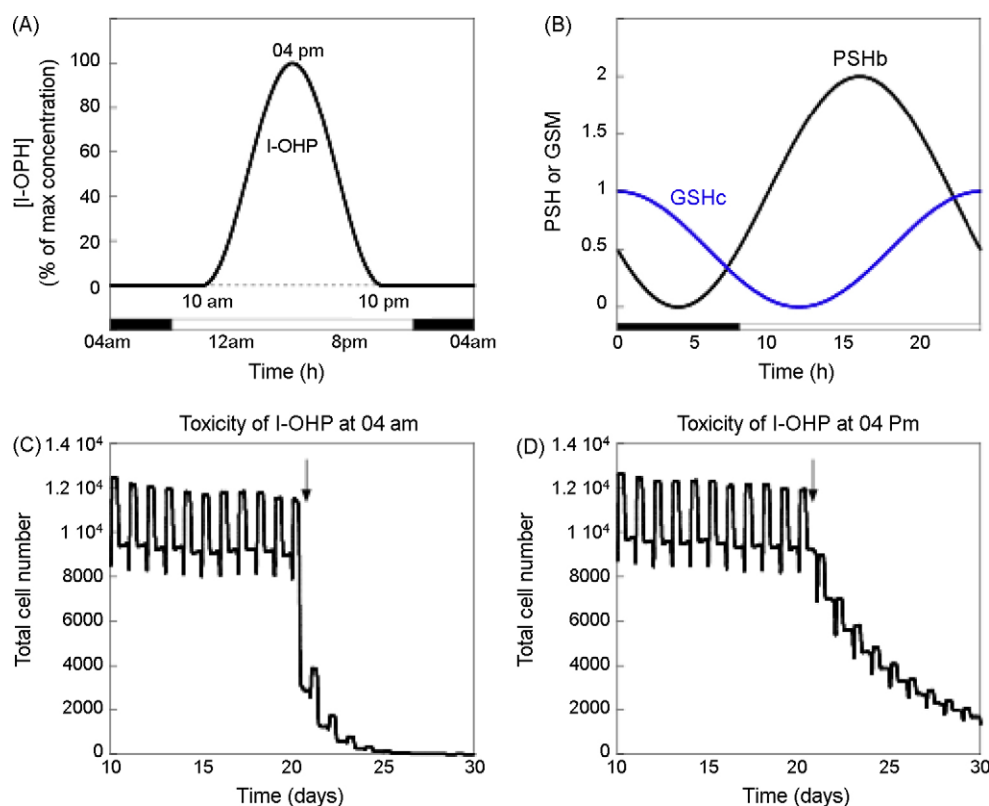


**Fig. 7 – Effect of circadian administration of oxaliplatin. (A)** The clinical chronoadministration of oxaliplatin occurs in antiphase of the previously described clinical administration of 5-FU. While the semi-sinusoidal variation of 5-FU has a peak time at 4 a.m. and is nil between 10 a.m. and 10 p.m., oxaliplatin is administered between this time span and reaches a maximum concentration at 4 p.m. The propensity for all cells to quit the proliferating pool increases with the drug concentration ([I-OHP]) according to Eq. (4) where  $k_{ox} = 0.09 \text{ acu}^{-1}$ . At the maximum of [I-OHP], equal to 100 acu, the exit propensity is thus multiplied by a factor of 10. **(B)** Circadian rhythms in plasma thiols (PSHb) and cellular glutathione (GSHc). PSHb seems to be predominant during the diurnal activity span with a peak time at 4 p.m. in the blood, and GSH reaches its maximum in the cell at the activity/rest transition, near midnight. **(C)** Time evolution of total cell number under circadian administration of I-OHP peaking at 4 a.m. The drug is chronoadministered from day 20 to day 30. The cell population suffers a large decrease due to the presence of the drug which kills the major part of the cell population within a few days. **(D)** Time evolution of total cell number under circadian administration of I-OHP peaking at 4 p.m. The drug is chronoadministered from day 20 to day 30. In this case, the drug kills a smaller part of the cell population owing to the reduction of the effective amount of free I-OHP that results from the formation of complexes with PSHb and GSHc.

rhythms, which play key roles in human physiology. Here we investigated the effect of circadian rhythms on chronotherapeutics with anticancer drugs by a complementary approach based on computational modeling. Thus, we used an automaton model for the cell cycle to probe the effects of circadian patterns of anticancer drug delivery. Two drugs were considered, one of which, 5-FU, exerts its cytotoxic effect at a particular phase of the cell cycle, while the other, oxaliplatin (I-OHP), kills cells at all cell cycle phases. In determining drug toxicity we took into account the possibility of entrainment of the cell cycle by the circadian clock.

The cell cycle automaton (CCA) model provides a convenient, versatile tool to determine the effect of various temporal patterns of drug administration. The automaton model describes the dynamic behavior of a single cell and of a cell population. It shows how a cell switches sequentially between the successive phases G1, S, G2 and M of the cell cycle.

After mitosis (M), two cells enter G1 and resume progression along the cell cycle. To ensure homeostasis, provision is made for cell death. When applying the CCA model to a population of cells, we consider that each phase of the cell cycle is characterized by a mean duration  $D$  and a variability  $V$ , so that the duration of each phase varies randomly in the interval  $D \pm V$ . Owing to such variability, the CCA model shows how a population of proliferating cells progressively desynchronizes until a steady state distribution of cell cycle phases is reached. Entrainment of the cell cycle by the circadian clock occurs via the circadian variation in the activity of the kinase WEE1, which prevents the G2/M transition; the peak in WEE1 is followed by a peak in the kinase CDK1. When introduced into the CCA model, the periodic variation in WEE1 and CDK1 allows us to account for entrainment of the cell cycle by the circadian clock. Thus, a cell cycle duration of 22 h can be extended to 24 h when the circadian variation in some of the model

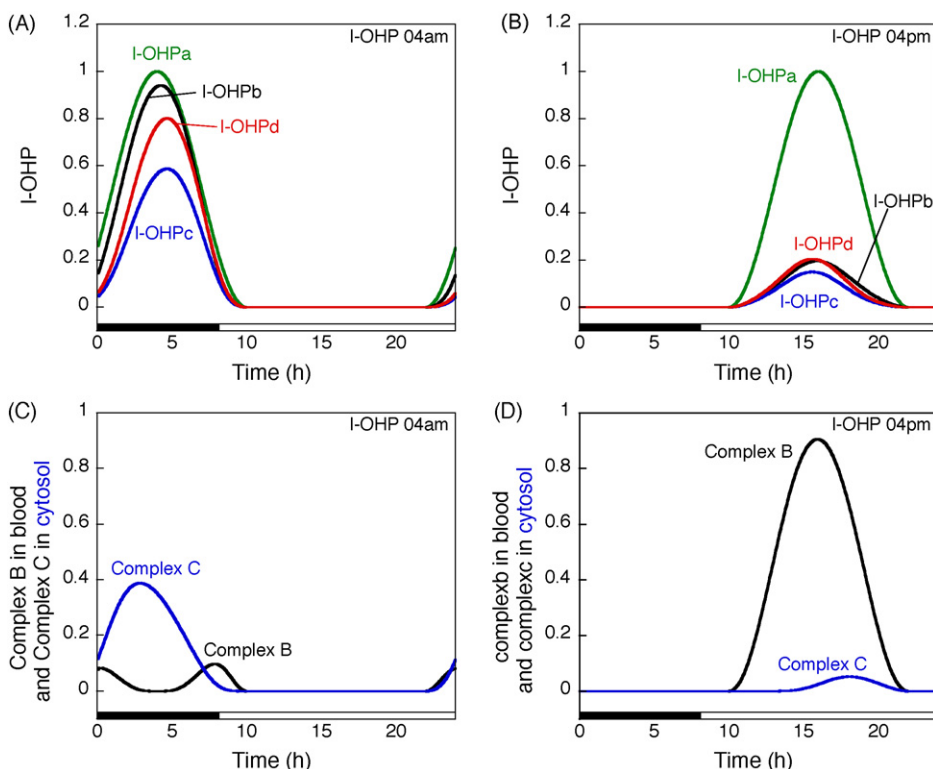


**Fig. 8** – Profiles of free l-OHP and l-OHP complexes associated with the chronoadministration of l-OHP at 4 a.m. (A and C) and 4 p.m. (B and D). (A) When l-OHP is administered (l-OHPa) at 4 a.m., both PSHb and GSHc are low, so that oxaliplatin in blood (l-OHPb) and in cells (l-OHPc) has a high enough concentration to allow build up of a large level of free l-OHP (l-OHPd) leading to cell death. (C) At 4 a.m., l-OHP is present during the through of PSH, thus avoiding the major mechanism of protection from l-OHP. Only cellular GSH can bind to the drug to form the inactive complex C. (B) At 4 p.m., chronoadministration results in the build up of only a small amount of free, toxic oxaliplatin (l-OHPd) that triggers cell death, due to the presence of PSH in plasma and GSH in cells and to the subsequent formation of relatively large amounts of inactive complexes B and C (see panel D). The curves are obtained by numerical integration of the kinetic equations listed in [Appendix A](#).

parameters is taken into account. Importantly, entrainment fixes the phase of the cell cycle with respect to the circadian clock, and, hence, with respect to the temporal pattern of drug administration.

Using numerical simulations of the CCA model, we first considered the case of 5-FU, which kills cells in S phase. We determined the effect of a circadian administration of the drug, according to the waveform shown in [Fig. 2A](#) and varied the time of peak delivery across a 24 h period. This analysis, performed for a cell cycle duration of 22 h, showed that the cytotoxicity of the drug is markedly affected by the temporal pattern of drug administration. Thus, a circadian pattern peaking at 4 a.m. is much more cytotoxic than a pattern peaking at 4 p.m. ([Fig. 2C](#) and [D](#)). The model allows us to clarify the reasons for such a differential effect according to the circadian pattern of drug administration. Key to this circadian dependence is the position of the temporal profile of the fraction of cells in S phase relative to the temporal pattern of the drug: cytotoxicity is minimum when the peak in 5-FU coincides with the minimum in the fraction of cells in S phase ([Fig. 2E](#)) and maximum when it coincides with the maximum in this fraction ([Fig. 2F](#)). Partial overlap of the temporal patterns of drug and fraction of cells in S phase occurs when

peak 5-FU delivery is shifted to other times of day, resulting in a histogram showing a clear minimum in cytotoxicity for peak delivery occurring around 3–4 a.m. ([Fig. 2B](#)). The CCA model further shows that both position and dip magnitude depend on the duration of the cycle prior to entrainment by the circadian clock. A clear minimum is seen only when the cell cycle duration prior to entrainment ranges from 18 to 26 h, and the minimum then shifts progressively from 12 p.m. to 12 a.m. However, the depth of the trough is most important when cell cycle duration ranges from 20 to 24 h. Then the minimum toxicity is observed around 1 a.m. to 5 a.m. This result supports the clinical use of a circadian pattern of 5-FU delivery peaking at 4 a.m. ([Lévi et al., 1994, 1997](#)).

We then considered the case of a second anticancer drug, oxaliplatin (l-OHP), which, in contrast to 5-FU, does not affect a specific phase of the cell cycle. Interestingly, the results show that a circadian dependence of cytotoxicity is also observed for this drug ([Figs. 7](#) and [9](#)). This finding corroborates the conclusions of a distinct mathematical approach based on the circadian control of oxaliplatin pharmacokinetics and pharmacodynamics ([Clairambault, 2007](#)). Here the model indicates that this circadian dependence originates from the circadian

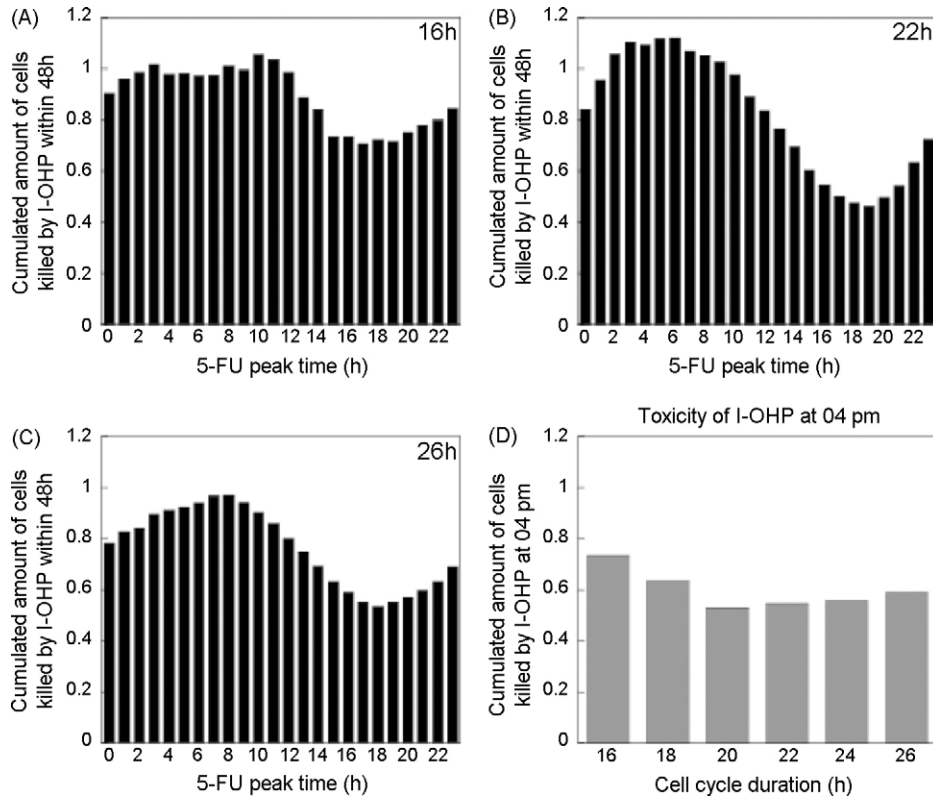


**Fig. 9 – Cytotoxicity of I-OHP as a function of peak time of circadian administration of the anticancer drug.** The cumulated amount of cells (in units of  $10^4$  cells) killed by I-OHP within 48 h is shown as a function of the peak time of circadian I-OHP administration for various durations of the cell cycle prior to entrainment: (A) 16 h, (B) 22 h, (C) 26 h. The results are obtained by means of the cell cycle automaton model for a variability  $V = 10\%$ . Minimal toxicity of oxaliplatin appears in each case when the circadian drug delivery pattern peaks near 16–18 h. The effect of the cell cycle length on the position of the minimum is less significant than in the case of 5-FU (compare with Fig. 3). (D) The least cytotoxic temporal pattern of I-OHP in (B) roughly retains the same cytotoxicity when the cell duration changes in the range 16–26 h, in contrast to the result obtained for 5-FU (Fig. 4D).

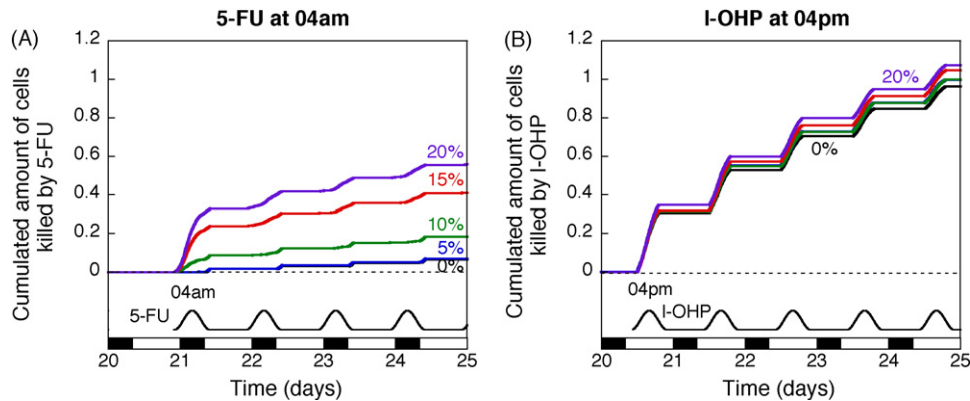


**Fig. 10 – Effect of variability in cell cycle phase durations.** (A) When 5-FU is administered according to a circadian pattern peaking at 4 a.m., the cumulated amount of cells killed by the drug increases with the variability  $V$  of cell cycle phase duration. (B) When I-OHP is administered according to a circadian pattern peaking at 4 p.m., the cumulated amount of cells killed by the drug increases only slightly with the variability of cell cycle phase durations. Prior to entrainment the cell cycle duration is 22 h. Curves are established for  $V$  ranging from 0% to 20%.

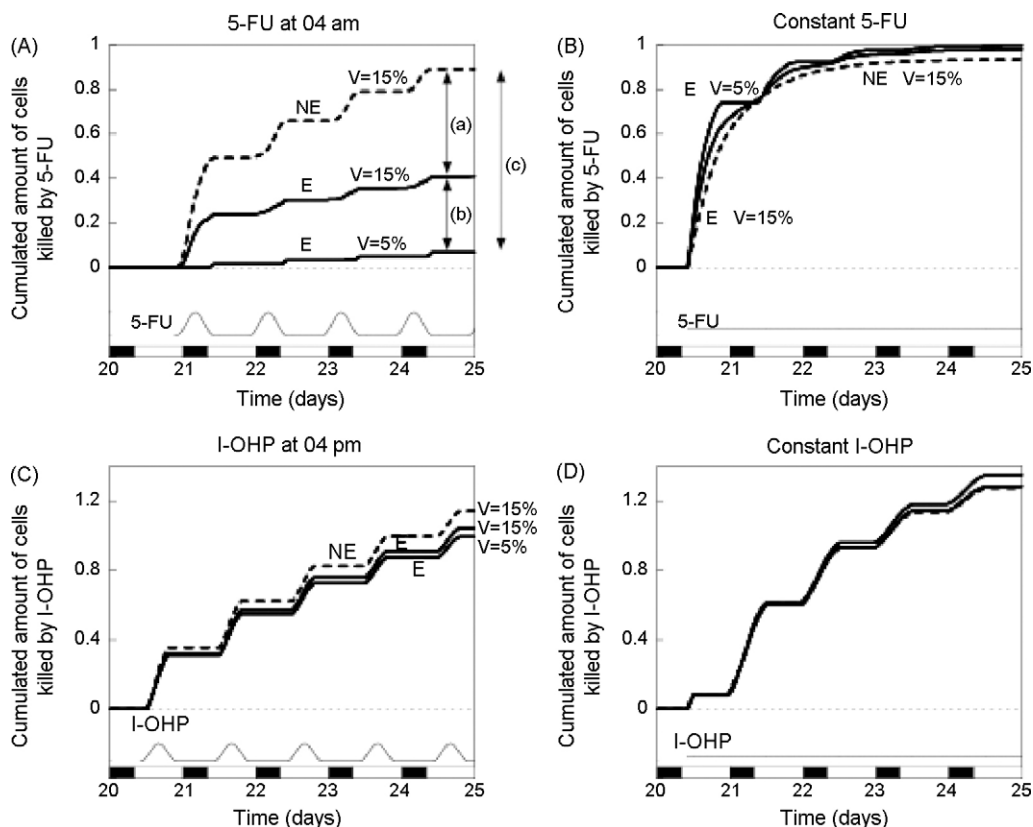


**Fig. 11** – Differential effects of circadian or continuous administration of 5-FU and oxaliplatin in cell populations differing by variability in cell cycle durations or/and entrainment by the circadian clock. (A) Comparison of cumulative cell kill (in units of  $10^4$  cells) upon circadian delivery of 5-FU peaking at 4 a.m. for two cell populations differing by variability  $V$  or/and by circadian entrainment. (a) The variability of the two populations is 15% but one is entrained (E) and the other not (NE). (b) Both populations are entrained by the circadian clock but the variabilities differ. (c) The first population is not entrained and the variability is 15%, the second one is entrained and the variability is 5%. (B) All the differences observed in (A) disappear when 5-FU is administered in a constant manner. The total quantity of drug delivered over 24 h is the same as in (A). (C) Comparison of cumulative cell kill (in units of  $10^4$  cells) by circadian delivery of I-OHP with a peak at 4 p.m. for two cell populations differing by variability  $V$ , equal to 5% or 15%, and by circadian entrainment (E or NE). Differential effects between populations with different variabilities, with or without circadian entrainment, do not occur with circadian administration of oxaliplatin, in contrast to what is observed in (A) for 5-FU. (D) Constant infusion of I-OHP does not show any differential effects and is equivalent to the most cytotoxic circadian administration pattern, which peaks at 4 a.m. (see Fig. 13B). Prior to entrainment the cell cycle duration in (A)–(D) is 22 h. Initial conditions correspond to the steady state distribution, (see Appendix A.4), except for cases where entrainment does not occur. Then all cells start at the beginning of G1.

variations of plasma thiols and cellular glutathione, which both form complexes with I-OHP and thereby reduce the amount of drug available for inflicting damage to the cells (Fig. 8). The magnitude of the minimum in the cytotoxicity histograms established for different values of the cell cycle duration prior to the entrainment by the circadian clock is, however, less pronounced than in the case of 5-FU (compare Fig. 9 with Fig. 3). The predictions of the CCA model nevertheless point to a minimum cytotoxicity of the temporal pattern of I-OHP delivery peaking near 4 p.m. to 6 p.m., which corresponds well to the circadian pattern of I-OHP delivery used clinically (Lévi et al., 1997). One further difference between the cases of 5-FU and I-OHP pertains to the effect of variability of cell cycle phase durations. In the case of 5-FU, an increase in such variability is accompanied by a rise in cytotoxicity, while

no much change in cytotoxicity is observed as a function of cell cycle variability for I-OHP (Fig. 10).

In searching for optimal patterns of anticancer drug delivery, two distinct goals must be pursued. Healthy tissues should be protected as much as possible from drug toxicity while attempting to cause at the same time maximum damage to the tumour. So far we determined drug toxicity in a single cell population, and focused on conditions corresponding to minimum cytotoxicity. The question arises as to how a temporal pattern ensuring maximum protection to healthy tissue could at the same time correspond to enhanced toxicity toward tumour cells. To investigate this question let us consider two populations of cells differing by one or more properties. The two populations can differ at least by cell cycle duration, variability in duration of the cell cycle phases, and/or entrainment

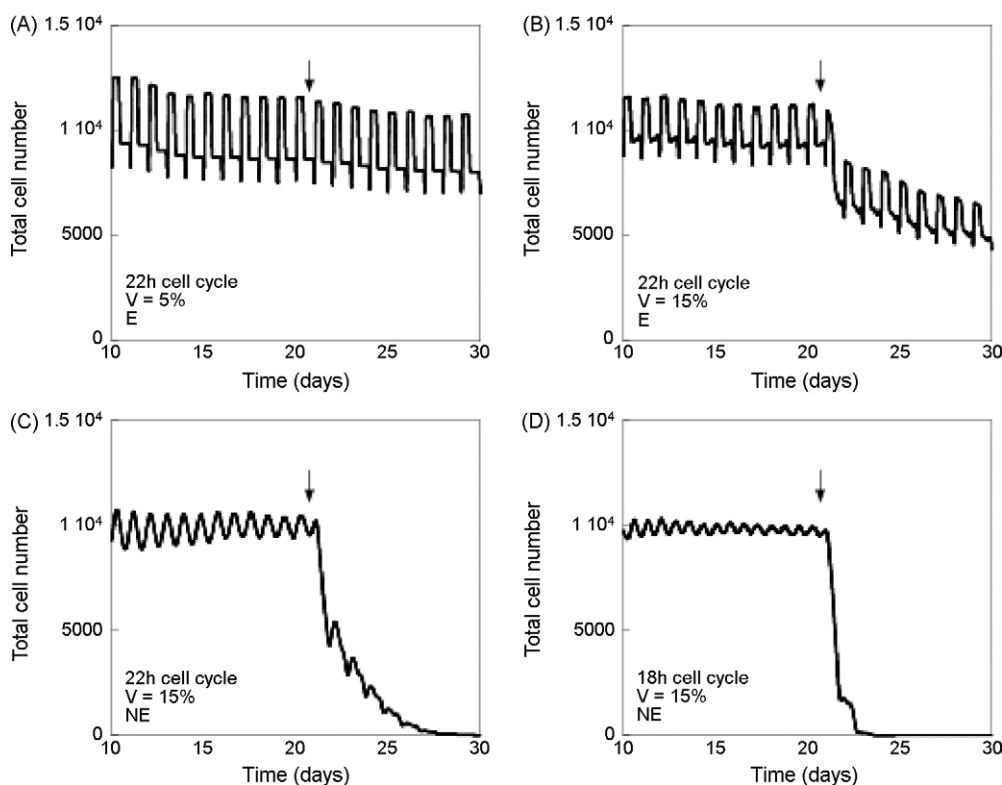


**Fig. 12 – The same circadian pattern of 5-FU administration can at the same time display minimum toxicity for one cell population (chronotolerance) and significant toxicity for a second cell population (chronefficacy). (A) Cell population with a cell cycle duration of 22 h and variability  $V = 5\%$ , entrained (E) by the circadian clock. (B) Same as (A) with variability  $V = 15\%$ . (C) Same as (B) without entrainment (NE) by the circadian clock. (D) Same as (C) with a cell cycle duration of 18 h. Comparison of cases (A) and (D) indicates strong cytotoxic effects of the same temporal pattern of 5-FU delivery when the two cell populations differ by properties such as entrainment by the circadian clock, variability in duration of cell cycle phases, and cell cycle duration.**

by the circadian clock, three factors which we have considered in our study. It is likely that additional differences between the normal and tumour cell populations exist.

Shown in Fig. 11A is the cytotoxicity over 5 successive days determined for the circadian pattern of 5-FU delivery peaking at 4 a.m., which is the least toxic one for a cell cycle duration of 22 h. The three curves show the evolution for a cell population entrained (E) by the circadian clock and characterized by a low variability ( $V = 5\%$ ), a second population entrained but characterized by a higher variability ( $V = 15\%$ ), and a third population with the same variability, but which is not entrained (NE) by the circadian clock. We observe a marked difference in cytotoxicity as a function of either factor (arrows marked (a) and (b) in Fig. 11A). The two factors are additive, thus the differential effect becomes larger when the two populations differ by both cell cycle variability and circadian entrainment. Such differential effects only occur for circadian administration of 5-FU and are not observed for constant 5-FU delivery (Fig. 11B), a schedule which is as cytotoxic as the circadian pattern peaking at 4 p.m. (see Fig. 3D and Altinok et al., 2007a; Altinok et al., 2007a,b). The differential cytotoxic effects predicted by the model for circadian administration of 5-FU as a function of circadian entrainment and variability is not observed for l-OHP, whether its delivery pattern is circadian or constant (Fig. 11C and D).

One further difference between the two cell populations pertains to the duration of the cell cycle prior to entrainment. Thus, if the normal cell population has a cell cycle duration of 22 h prior to entrainment and if the tumour cell population has a different cell cycle duration, then the circadian pattern of drug delivery peaking at 4 a.m., which is least cytotoxic to the normal population, will be more cytotoxic toward the second population (see Fig. 4D). A similar, though weaker effect, is predicted in the case of l-OHP (Fig. 9D).

That chronefficacy may coincide with chronotolerance is further illustrated in Fig. 12 for 5-FU. Here, the same temporal pattern of drug delivery peaking at 4 a.m. is applied to two populations differing either by the variability in durations of cell cycle phases, the capacity of being entrained by the circadian clock, the duration of the cell cycle. Maximum differential effects are obtained when the two populations differ by the three characteristics (compare Fig. 12A and D).

In establishing the cytotoxicity histograms (Figs. 3, 4D, and 9) we measured cytotoxicity as the cumulated amount of cells killed by 5-FU or l-OHP over 48 h. As shown in Fig. 2E and F, the most significant decrease in the number of cells due to killing by 5-FU indeed occurs within the first two days of treatment. We have nevertheless established the time course of cytotoxicity over a longer period of 5 days (see Figs. 11 and 12), which period matches the typical duration

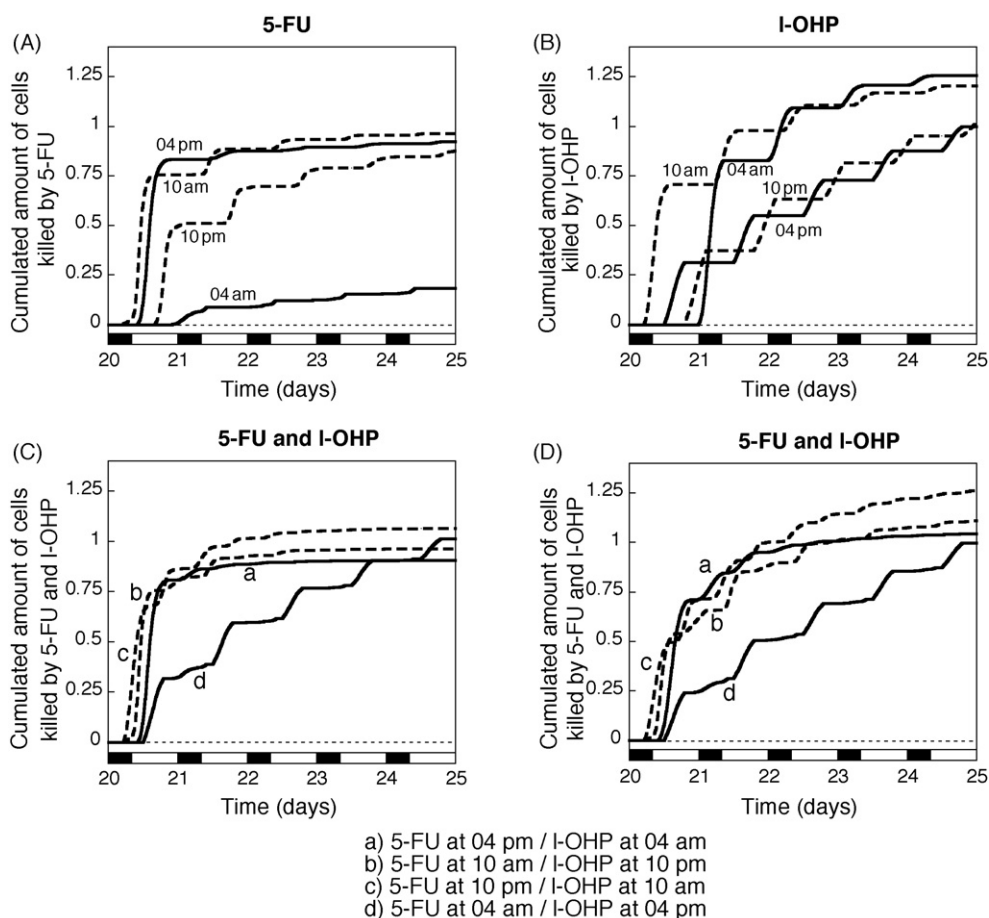


**Fig. 13** – Effect of circadian administration of 5-FU or l-OHP alone compared with a combined chronotherapy by the two drugs. (A) Toxicity for circadian schedules of 5-FU delivery peaking at various times (4 a.m., 10 a.m., 4 p.m. and 10 p.m.), when variability  $V$  is equal to 10%. The less toxic chronoadministration occurs when 5-FU has a peak time at 4 a.m. (B) Toxicity for circadian schedules of oxaliplatin delivery peaking at various times (4 a.m., 10 a.m., 4 p.m. and 10 p.m.), when variability  $V$  is equal to 10%. The less toxic chronoadministration occurs when oxaliplatin has a peak time at 4 p.m. (C) Toxicity for circadian schedules of 5-FU delivery peaking at various times (4 a.m., 10 a.m., 4 p.m. and 10 p.m.), combined with circadian patterns of oxaliplatin delivered at corresponding times shifted by 12 h, when variability  $V$  is equal to 10%. Due to the combined action of the two anticancer drugs, the total cell kill for curve d is higher than with the sole administration of 5-FU. The less toxic pattern of combined administration of the two drugs is a composite of the less toxic patterns of chronoadministration observed in (A) for 5-FU delivery peaking at 4 a.m. and in (B) for oxaliplatin delivery peaking at 4 p.m. (D) A similar result is also observed with half of the doses of 5-FU and l-OHP administered in (C).

of a session of chronotherapy. In the chronotherapeutics of metastatic colorectal cancer, 5-FU and l-OHP were administered in a circadian manner during courses of 4 or 5 days, separated with respective treatment-free intervals of 10 or 16 days (Lévi et al., 1997; Lévi, 2001).

So far the cytotoxic effects of 5-FU and l-OHP have been determined independently in our model. In clinical treatment, however, both drugs are combined, each with its own circadian delivery pattern (peaking at 4 a.m. for 5-FU and at 4 p.m. for l-OHP). The question thus arises as to whether and how the results obtained for each anticancer drug independently are affected by the other drug. It is useful to address this question as well as the effect of reducing the quantity of drugs administered in such conditions. Shown in Fig. 13 are the cytotoxicity time course over 5 days for both 5-FU (panel A) and l-OHP (panel B). The results confirm those reported for cumulated

cytotoxicity determined over 48 h in Figs. 2 and 3 for 5-FU, and 7 and 9 for l-OHP. For a cell cycle duration of 22 h prior to entrainment by the circadian clock, the minimum cytotoxicity is observed for a circadian pattern peaking at 4 a.m. for 5-FU and at 4 p.m. for l-OHP. The difference between the four patterns of 5-FU delivery (peaks at 4 a.m., 10 a.m., 4 p.m., or 10 p.m.) in Fig. 13A is more important than that observed for l-OHP in Fig. 13B. When the two drugs are administered together, without changing their quantity, the propensity of quitting the cell cycle at the S phase is given by Eq. (5):

$$P = P_0(1 + k_f[5\text{-FU}] + k_{ox}[l\text{-OHP}]) \quad (5)$$

while the propensity of exiting the proliferative compartment in other phases of the cycle is given by Eq. (4).

The results on the combined administration of 5-FU and l-OHP indicate that the four conditions separate into two groups (Fig. 13C). The least cytotoxic delivery pattern combines circadian delivery with peaks at 4 a.m. for 5-FU and at 4 p.m. for l-OHP. More cytotoxic are the patterns in which circadian delivery peaks at 4 p.m., 10 p.m., or 10 a.m. for 5-FU and at 4 a.m., 10 a.m., or 10 p.m. for l-OHP, respectively. The differences between the four circadian patterns of the combination persist when the dose levels of each drug are halved. The least cytotoxic pattern combines the characteristics of minimum cytotoxicity observed for each drug independently, namely the pattern in which the circadian delivery peaks at 4 a.m. for 5-FU and at 4 p.m. for l-OHP. In panels C and D we note that owing to the combined cytotoxicity of 5-FU and l-OHP, a similar amount of cells are killed after 5 days. The differences are most noticeable during the first 2 to 3 days of chronotherapy.

The automaton model for the cell cycle thus provides a useful tool for assessing the cytotoxic effect of various temporal patterns of anticancer drug delivery. Although the model is relatively simple and does not take into account explicitly the detailed molecular machinery controlling cell proliferation, it nevertheless shows how a population of cells can progressively desynchronize due to the stochastic nature of the transitions between the successive phases of the cell cycle and the variability that characterizes their duration. The results obtained by numerical simulations of the cell cycle automaton indicate that the least cytotoxic patterns of 5-FU and l-OHP circadian administration match those used clinically. The model therefore corroborates the use of such patterns that were initially selected on the basis of experimental studies in animals, and subsequently tested in humans. The model shows that continuous administration of 5-FU and l-OHP has the same effect as the most cytotoxic circadian pattern of drug delivery. Additionally the model helps us identify factors that may contribute to explain a long-standing puzzle, namely, why temporal patterns corresponding to minimum cytotoxicity for a population of healthy cells could at the same time prove more cytotoxic toward a population of tumour cells.

## Acknowledgments

This work was supported by the European Union through the Network of Excellence BioSim, Contract No. LSHB-CT-2004-005137, by grant no. 3.4607.99 from the *Fonds de la Recherche Scientifique Médicale* (F.R.S.M., Belgium), and by the Belgian Federal Science Policy Office (IAP P6/25 “BioMaGNet”: “Bioinformatics and Modeling- From Genomes to Networks”).

## Appendix A

### A.1. Scheme of the automaton model for the cell cycle, incorporating the effect of chronotherapy by 5-FU and oxaliplatin (l-OHP)

The scheme details the successive steps performed by the automaton model along the successive phases of the cell cycle (see Fig. A.1).

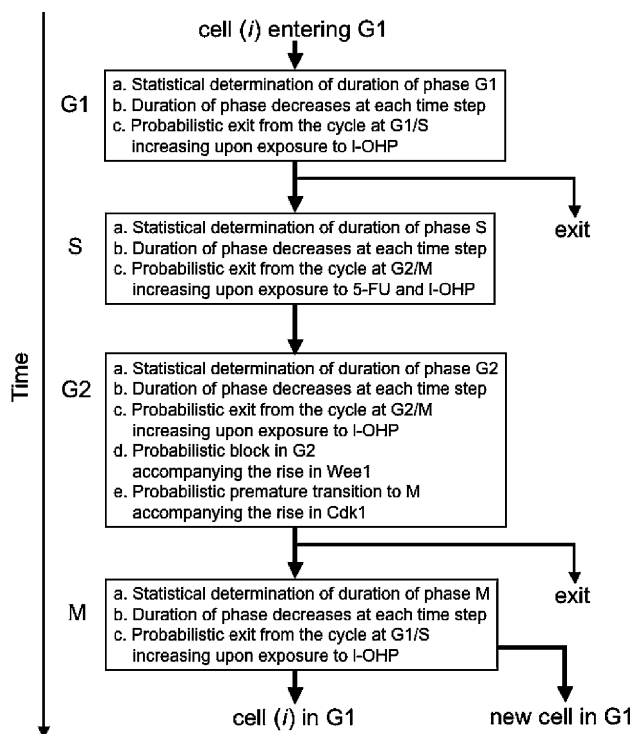


**Fig. A.1 – Detailed steps followed by the automaton model as it progresses along the successive phases of the cell cycle.**

### A.2. Ensuring homeostasis of the cell population in the cell cycle automaton model

In order to stabilize the cell population around  $10^4$  cells, which is the typical number of cells considered in numerical simulations, the logistic Eq. (A.1) incorporating the total cell number of cells,  $N$ , describes the time evolution of the propensity  $P$  to quit the proliferating pool:

$$P = P_0 + k_s \left( \frac{N}{N_s} - 1 \right) \quad (\text{A.1})$$

with  $k_s = 10^{-4} \text{ min}^{-1}$  and  $N_s = 10^4$  cells. When the population is above  $N_s$ , the propensity to quit the cell cycle increases to stabilize the population around the steady-state value  $N_s = 10^4$  cells. Conversely, this propensity decreases when the population is under  $N_s$ .

### A.3. Kinetic equations for the formation of oxaliplatin complexes with plasma thiols and glutathione

When applying the CCA model to the case of 5-FU, we assume that the effective concentration of 5-FU at the site of action is given by the circadian profile of drug delivery. We then determine the increased propensity to quit the cell cycle owing to the toxicity of 5-FU. In contrast, for oxaliplatin, because this compound forms complexes with PSH and GSH, before determining the increased propensity to exit the cell cycle due to the action of the drug we must first determine the effective, free concentration of l-OHP after formation of complexes with PSH and GSH. The time evolution of the various forms of l-OHP is given, according to the scheme of Fig. 6B, by the kinetic Eq. (A.2) where  $OHP_b$ ,  $OHP_c$ ,  $OHP_d$ , denote, respectively, the

concentrations of l-OHP in blood, l-OHP cytosolic concentration, and the effective l-OHP concentration exerting damage to DNA;  $PSH_b$  and  $GSH_c$  denote the concentrations of plasma thiol and cellular glutathione;  $Complex_b$  and  $Complex_c$  denote the concentrations of the complexes formed by oxaliplatin with plasma thiols and cellular glutathione, respectively. The various rate constants are defined in the scheme of Fig. 6B; parameters  $kd_1$ ,  $kd_2$ ,  $kd_3$ ,  $kd_p$ ,  $kd_g$ ,  $kd_{c1}$ , and  $kd_{c2}$  are degradation rates.

$$\begin{aligned} \frac{dOHP_b}{dt} &= k_0OHP_a - kd_1OHP_b - kc_1OHP_bPSH_b^2 \\ &\quad - k_1OHP_b + k_{11}OHP_c \\ \frac{dOHP_c}{dt} &= k_1OHP_b - kd_2OHP_c - kc_2OHP_cGSH_c^2 \\ &\quad - k_2OHP_c - k_{11}OHP_c + k_{22}OHP_d \\ \frac{dOHP_d}{dt} &= k_2OHP_c - kd_3OHP_d - k_{22}OHP_d \\ \frac{dPSH_b}{dt} &= k_pPSH - kd_pPSH_b - kc_1OHP_bPSH_b^2 \\ \frac{dGSH_c}{dt} &= k_gGSH - kd_gGSH_c - kc_2OHP_cGSH_c^2 \\ \frac{dComplex_b}{dt} &= kc_1OHP_bPSH_b^2 - kd_{c1}Complex_b \\ \frac{dComplex_c}{dt} &= kc_2OHP_cGSH_c^2 - kd_{c2}Complex_c \end{aligned} \quad (A.2)$$

Prior to running numerical simulations of the cell cycle automaton model in the case of chronotherapy by oxaliplatin, we determine the various forms of l-OHP by numerical integration of Eqs. (A.2) and obtain the time variation of the form  $OHP_d$ . The latter is used for computing the propensity of quitting the cell cycle owing to the cytotoxic effect of l-OHP.

Simulations were performed using the following numerical values which were selected in an arbitrary manner so as to yield a half-time of l-OHP of the order of 10 min (Lévi et al., 2000) and a sufficiently rapid time course for the formation of l-OHP complexes with PSH and GSH:

$$\begin{aligned} k_0 &= 100 \text{ h}^{-1} \\ k_1 &= 125 \text{ h}^{-1}, & k_{11} &= 80 \text{ h}^{-1}, & kd_1 &= 30 \text{ h}^{-1} \\ k_2 &= 150 \text{ h}^{-1}, & k_{22} &= 80 \text{ h}^{-1}, & kd_2 &= 30 \text{ h}^{-1} \\ k_p &= 100 \text{ h}^{-1}, & kd_p &= 90 \text{ h}^{-1} \\ k_g &= 100 \text{ h}^{-1}, & kd_g &= 90 \text{ h}^{-1} \\ kc_1 &= 240 \text{ acu}^{-2} \text{ h}^{-1}, & kd_{c1} &= 90 \text{ h}^{-1} \\ kc_2 &= 240 \text{ acu}^{-2} \text{ h}^{-1}, & kd_{c2} &= 90 \text{ h}^{-1} \end{aligned}$$

#### A.4. Parameter values for numerical simulations of the cell cycle automaton model

(A) Parameter values for the 22 h cell cycle under circadian entrainment (with  $k_w = 0.015 \text{ acu}^{-1} \text{ min}^{-1}$  and  $k_c = 0.001 \text{ acu}^{-1} \text{ min}^{-1}$ ).

Variability	$P_0$ ( $\text{min}^{-1}$ )	Figures
$V=0\%$	$0.4925 \times 10^{-3}$	10
$V=5\%$	$0.4930 \times 10^{-3}$	10–12A
$V=10\%$	$0.5000 \times 10^{-3}$	2B–D; 3D; 4B, D; 7C, D; 9B, D; 10
$V=15\%$	$0.5125 \times 10^{-3}$	2E, F; 10; 11; 12B
$V=20\%$	$0.5230 \times 10^{-3}$	10

Initial conditions:  $10^4$  cells at steady state (see D).

(B) Parameter values for other cell cycle durations under circadian entrainment (with a variability  $V=10\%$ ).

Cell cycle	$P_0$ ( $\text{min}^{-1}$ )	$k_w$ ( $\text{acu}^{-1} \text{ min}^{-1}$ )	$k_c$ ( $\text{acu}^{-1} \text{ min}^{-1}$ )	Figures
16 h	$0.7230 \times 10^{-3}$	0.300	0.001	3A; 4A, D; 9A
18 h	$0.5515 \times 10^{-3}$	0.300	0.001	3B; 4D; 9D
20 h	$0.4920 \times 10^{-3}$	0.300	0.001	3C; 4D; 9D
24 h	$0.4920 \times 10^{-3}$	0.015	0.001	3E; 4D; 9D
26 h	$0.4620 \times 10^{-3}$	0.015	0.015	3F; 4D; 9C, D; 10C

Initial conditions:  $10^4$  cells at steady state (see D).

(C) Parameter values for cell cycle durations without circadian entrainment.

Cell cycle	Variability	$P_0$ ( $\text{min}^{-1}$ )	Figures
18 h	15%	$0.6620 \times 10^{-3}$	12D
22 h	15%	$0.5380 \times 10^{-3}$	11, 12C

Initial conditions:  $10^4$  cells beginning G1.

(D) Steady-state distribution of cell cycle phases for the different cell cycle durations.

Cell cycle	Duration in G1, S, G2, M	Initial condition for $10^4$ cells (steady state distribution)
16 h	3 h, 11 h, 1 h, 1 h	2527 in G1, 6417 in S, 583 in G2, 428 in M
18 h	5 h, 11 h, 1 h, 1 h	3656 in G1, 5480 in S, 498 in G2, 366 in M
20 h	7 h, 11 h, 1 h, 1 h	4465 in G1, 4781 in S, 435 in G2, 319 in M
22 h	9 h, 11 h, 1 h, 1 h	5091 in G1, 4240 in S, 386 in G2, 283 in M
24 h	11 h, 11 h, 1 h, 1 h	5589 in G1, 3810 in S, 346 in G2, 254 in M
26 h	13 h, 11 h, 1 h, 1 h	5996 in G1, 3459 in S, 314 in G2, 231 in M

#### REFERENCES

- Altinok, A., Lévi, F., Goldbeter, A., 2007a. A cell cycle automaton model for probing circadian patterns of anticancer drug delivery. *Adv. Drug Deliv. Rev.* 59, 1036–1053.
- Altinok, A., Lévi, F., Goldbeter, A., 2007b. Optimizing temporal patterns of anticancer drug delivery by simulations of a cell cycle automaton. In: Bertau, M., Mosekilde, E., Westerhoff, H.V. (Eds.), *Biosimulation in Drug Development*. Wiley-VCH, Weinheim, pp. 275–297.
- Bjarnason, G.A., Jordan, R., 2000. Circadian variation of cell proliferation and cell cycle protein expression in man: clinical implications. *Prog. Cell Cycle Res.* 4, 193–206.
- Bjarnason, G.A., Jordan, R.C.K., Wood, P.A., Li, Q., Lincoln, D.W., Sothorn, R.B., Hrushesky, W.J.M., Ben-David, Y., 2001. Circadian expression of clock genes in human oral mucosa and skin. *Am. J. Pathol.* 158, 1793–1801.

- Boughattas, N., Lévi, F., Fournier, C., Lemaigre, G., Roulon, A., Hecquet, B., Mathé, G., Reinberg, A., 1989. Circadian rhythms in toxicities and tissues uptake of oxaliplatin in mice. *Cancer Res.* 49, 3362–3368.
- Bridges, A.B., Fisher, T.C., Scott, N., McLaren, M., Belch, J.J.F., 1992. Circadian rhythm of white blood cell aggregation and free radical status in healthy volunteers. *Free Radic. Res. Commun.* 16, 89–97.
- Brooks, R.F., Bennett, D.C., Smith, J.A., 1980. Mammalian cell cycles need two random transitions. *Cell* 19, 493–504.
- Burns, E.R., Beland, S.S., 1984. Effect of biological time on the determination of the LD50 of 5-fluorouracil in mice. *Pharmacology* 28, 296–300.
- Cain, S.J., Chau, P.C., 1997. Transition probability cell cycle model. I. Balanced growth. *J. Theor. Biol.* 185, 55–67.
- Clairambault, J., 2007. Modelling oxaliplatin drug delivery to circadian rhythms in drug metabolism and host tolerance. *Adv. Drug Deliv. Rev.* 59, 1054–1068.
- El Kouni, M.H., Naguib, F.N.M., Park, K.S., Cha, S., Darnowski, J.W., Soong, S.J., 1990. Circadian rhythm of hepatic uridine phosphorylase activity and plasma concentration of uridine in mice. *Biochem. Pharmacol.* 40, 2479–2485.
- Filipski, E., Innominato, P., Wu, M., Li, X.M., Iacobelli, S., Xian, L.J., Lévi, F., 2005. Effects of light and food schedules on liver and tumor molecular clocks in mice. *J. Natl. Cancer Inst.* 97, 507–517.
- Focan, C., 2003. Rhythms of cancer chemotherapy. In: Redfern, P. (Ed.), *Chronotherapeutics*. Pharmaceutical Press, London, Chicago, pp. 235–282.
- Fu, L., Pelicano, H., Liu, J., Huang, P., Lee, C., 2002. The circadian gene *Period2* plays an important role in tumor suppression and DNA damage response in vivo. *Cell* 111, 41–50.
- Gachon, F., Olela, F., Schaad, O., Descombes, P., Schibler, U., 2006. The circadian PAR-domain basic leucine zipper transcription factors DBP, TEF and HLF modulate basal and inducible xenobiotic detoxification. *Cell Metab.* 4, 25–36.
- Gery, S., Komatsu, N., Baldjyan, L., Yu, A., Koo, D., Koeffler, H., 2006. The circadian gene *per1* plays an important role in cell growth and DNA damage control in human cancer cells. *Mol. Cell* 22, 375–382.
- Goldbeter, A., Claude, D., 2002. Time-patterned drug administration: insights from a modeling approach. *Chronobiol. Int.* 19, 157–175.
- Granda, T., Lévi, F., 2002. Tumor based rhythms of anticancer efficacy in experimental models. *Chronobiol. Int.* 19, 21–41.
- Granda, T.G., D'Attino, R.M., Filipiński, E., Vrignaud, P., Garufi, C., Terzoli, E., Bissery, M.C., Lévi, F., 2002. Circadian optimization of irinotecan and oxaliplatin efficacy in mice with Glasgow osteosarcoma. *Brit. J. Cancer* 86, 999–1005.
- Granda, T.G., Liu, X.H., Smaaland, R., Cermakian, N., Filipiński, E., Sassone-Corsi, P., Lévi, F., 2005. Circadian regulation of cell cycle and apoptosis proteins in mouse bone marrow and tumour. *FASEB J.* 19, 304–306.
- Harris, B.E., Song, R., Soong, S.J., Diasio, R.B., 1990. Relationship between dihydropyrimidine dehydrogenase activity and plasma 5-fluorouracil levels with evidence for circadian variation of enzyme activity and plasma drug levels in cancer patients receiving 5-fluorouracil by protracted continuous infusion. *Cancer Res.* 50, 197–201.
- Haus, E., Halberg, F., Pauly, J.E., Cardoso, S., Kühl, J.F., Sothorn, R.B., Shiotsuka, R.N., Hwang, D.S., 1972. Increased tolerance of leukemic mice to arabinosyl cytosine with schedule adjusted to circadian system. *Science* 177, 80–82.
- Hirayama, J., Cardone, L., Doi, M., Sassone-Corsi, P., 2005. Common pathways in circadian and cell cycle clocks: light-dependent activation of Fos/AP-1 in zebrafish controls CRY-1a and WEE-1. *Proc. Natl Acad. Sci. U.S.A.* 102, 10194–10199.
- Hrushesky, W.J., Lévi, F.A., Halberg, F., Kennedy, B.J., 1982. Circadian stage dependence of cis-diamminedichloroplatinum lethal toxicity in rats. *Cancer Res.* 42, 945–949.
- Lévi, F., 1997. Chronopharmacology of anticancer agents. In: Redfern, P.H., Lemmer, B. (Eds.), *Physiology and Pharmacology of Biological Rhythms (Handbook of Experimental Pharmacology)*, vol. 125. Springer-Verlag, Berlin, pp. 299–331.
- Lévi, F., 2001. Circadian chronotherapy for human cancers. *Lancet Oncol.* 2, 307–315.
- Lévi, F., 2008. Personalized chronotherapeutics of cancer. The Endocrine Society's 90th Annual Meeting, ENDO 2008, June 15–18, 2008, San Francisco, USA, Abstract S24-3, p. 42.
- Lévi, F., Altinok, A., Clairambault, J., Goldbeter, A., 2008. Implications of circadian clocks for the rhythmic delivery of cancer therapeutics. *Philos. Trans. A: Math. Phys. Eng. Sci.* 366, 3575–3598.
- Lévi, F., Filipiński, E., Iurisci, I., Li, X.M., Innominato, P., 2007a. Crosstalks between circadian timing system and cell division cycle determine cancer biology and therapeutics. *Cold Spring Harb Symp. Quant. Biol.* 72, 465–475.
- Lévi, F., Focan, C., Karaboué, A., de la Valette, V., Focan-Henrard, D., Baron, B., Kreutz, M., Giacchetti, S., 2007b. Implications of circadian clocks for the rhythmic delivery of cancer therapeutics. *Adv. Drug Deliv. Rev.* 59, 1015–1035.
- Lévi, F., Metzger, G., Massari, C., Milano, G., 2000. Oxaliplatin: pharmacokinetics and chronopharmacological aspects. *Clin. Pharmacokinet.* 38, 1–21.
- Lévi, F., Schibler, U., 2007. Circadian rhythms: mechanisms and therapeutic implications. *Annu. Rev. Pharmacol. Toxicol.* 47, 593–628.
- Lévi, F., Zidani, R., Vannetzel, J.M., Perpoint, B., Focan, C., Faggiuolo, R., Chollet, P., Garufi, C., Itzhaki, M., Dogliotti, L., 1994. Chronomodulated versus fixed-infusion-rate delivery of ambulatory chemotherapy with oxaliplatin, fluorouracil, and folinic acid (leucovorin) in patients with colorectal cancer metastases: a randomized multi-institutional trial. *J. Natl. Cancer Inst.* 86, 1608–1617.
- Lévi, F., Zidani, R., Misset, J.L., 1997. Randomised multicentre trial of chronotherapy with oxaliplatin, fluorouracil, and folinic acid in metastatic colorectal cancer. *International Organization for Cancer Chronotherapy. Lancet* 350, 681–686.
- Li, X.M., Metzger, G., Filipiński, E., Lemaigre, G., Lévi, F., 1998. Modulation of nonprotein sulphhydryl compounds rhythm with buthionine sulphoximine: relationship with oxaliplatin toxicity in mice. *Arch. Toxicol.* 72, 574–579.
- Li, X.M., Kanekal, S., Crépin, D., Guettier, C., Carrière, J., Elliott, G., Lévi, F., 2006. Circadian pharmacology of L-alanosine (SDX-102) in mice. *Mol. Cancer Ther.* 5, 337–346.
- Matsuo, T., Yamaguchi, S., Mitsui, S., Emi, A., Shimoda, F., Okamura, H., 2003. Control mechanism of the circadian clock for timing of cell division in vivo. *Science* 302, 255–259.
- Metzger, G., Massari, C., Etienne, M.C., 1994. Spontaneous or imposed circadian changes in plasma concentrations of 5-fluorouracil coadministered with folinic acid and oxaliplatin: relationship with mucosal toxicity in cancer patients. *Clin. Pharm. Ther.* 56, 190–201.
- Naguib, F.N., Soong, S.J., El Kouni, M.H., 1993. Circadian rhythm of orotate phosphoribosyltransferase, pyrimidine nucleoside phosphorylases and dihydrouracil dehydrogenase in mouse liver. Possible relevance to chemotherapy with 5-fluoropyrimidines. *Biochem. Pharmacol.* 45, 667–673.
- Nowakowska-Dulawa, E., 1990. Circadian rhythm in 5-fluorouracil (FU) pharmacokinetics and tolerance. *Chronobiologia* 17, 27–35.
- Ohdo, S., Koyanagi, S., Suyama, H., Higuchi, S., Aramaki, H., 2001. Changing the dosing schedule minimizes the disruptive effects of interferon on clock function. *Nature Med.* 7, 356–360.

- Peters, G.J., Van Dijk, J., Nadal, J.C., Van Groeningen, C.J., Lankelma, J., Pinedo, H.M., 1987. Diurnal variation in the therapeutic efficacy of 5-fluorouracil against murine colon cancer. *In Vivo* 1, 113–117.
- Petit, E., Milano, G., Lévi, F., Thyss, A., Bailleul, F., Schneider, M., 1988. Circadian varying plasma concentration of 5-FU during 5-day continuous venous infusion at constant rate in cancer patients. *Cancer Res.* 48, 1676–1679.
- Popovic, P., Popovic, V., Baughman, J., 1982. Circadian rhythm and 5-fluorouracil toxicity in C3H mice. *Prog. Clin. Biol. Res.* 107, 185–187.
- Porsin, B., Formento, J.L., Filipski, E., Etienne, M.C., Francoual, M., Renée, N., Lévi, F., Milano, G., 2003. Dihydropyrimidine dehydrogenase circadian rhythm in both enzyme activity and gene expression from mouse liver. *Eur. J. Cancer* 39, 822–828.
- Reddy, A.B., Wong, G.K.Y., O'Neill, J., Maywood, E.S., Hastings, M.H., 2005. Circadian clocks: neural and peripheral pacemakers that impact upon the cell division cycle. *Mutat. Res.* 574, 76–91.
- Smaaland, R., Sothorn, R.B., Laerum, O.D., Abrahamsen, J.F., 2002. Rhythms in human bone marrow and blood cells. *Chronobiol. Int.* 19, 101–127.
- Smith, J.A., Martin, L., 1973. Do cells cycle? *Proc. Natl. Acad. Sci. U.S.A.* 70, 1263–1267.
- Tampellini, M., Filipski, E., Liu, X.H., Lemaigre, G., Li, X.M., Vrignaud, P., François, E., Bissery, M.C., Lévi, F., 1998. Docetaxel chronopharmacology in mice. *Cancer Res.* 58, 3896–3904.
- Voland, C., Bord, A., Péleraux, A., Pénarier, G., Carrière, D., Galiègue, S., Cvitkovic, E., Jbilo, O., Casellas, P., 2006. Repression of cell cycle-related proteins by oxaliplatin but not cisplatin in human colon cancer cells. *Mol. Cancer Ther.* 5, 2149–2157.
- Wood, P.A., Du-Quiton, J., You, S., Hrushesky, W.J., 2006. Circadian clock coordinates cancer cell cycle progression, thymidylate synthase, and 5-fluorouracil therapeutic index. *Mol. Cancer Ther.* 8, 2023–2033.
- Wu, M.W., Xian, L.J., Li, X.M., Innominato, P., Lévi, F., 2004. Circadian expression of dihydropyrimidine dehydrogenase, thymidylate synthase, c-myc and p53 mRNA in mouse liver tissue. *Ai Zheng* 23, 235–242.
- Zeng, Z.L., Sun, J., Guo, L., Li, S., Wu, M.W., Qiu, F., Jiang, W.Q., Lévi, F., Xian, L.J., 2005. Circadian rhythm in dihydropyrimidine dehydrogenase activity and reduced glutathione content in peripheral blood of nasopharyngeal carcinoma patients. *Chronobiol. Int.* 22, 741–754.
- Zhang, R., Lu, Z., Liu, T., Soong, S.J., Diasio, R.B., 1993. Relationship between circadian dependent toxicity of 5-fluorodeoxyuridine and circadian rhythms of pyrimidine enzymes: possible relevance to fluoropyrimidine chemotherapy. *Cancer Res.* 53, 2816–2822.